

EFFECTS OF ZINC OXIDE ON THERMAL, MECHANICAL, MORPHOLOGICAL, AND GAS
BARRIER PROPERTIES OF POLYBUTYLENE SUCCINATE/ POLY(3-HYDROXYBUTYRATE-CO-
4-HYDROXYBUTYRATE) FILMS



A Thesis Submitted in Partial Fulfillment of the Requirements
for the Degree of Master of Engineering in Chemical Engineering

Department of Chemical Engineering

FACULTY OF ENGINEERING

Chulalongkorn University

Academic Year 2022

Copyright of Chulalongkorn University

ผลกระทบของซิงค์ออกไซด์ที่มีผลต่อคุณสมบัติทางความร้อน ทางกล ทางสัณฐานวิทยา และการ
ต้านทานการซึมผ่านของก๊าซ ของฟิล์มพอลิเมอร์ผสมระหว่างพอลิบิวทิลีนซัคซิเนต และพอลิ(3-ไฮดรอกซีบิวทิเรต-โค-4-ไฮดรอกซีบิวทิเรต)



วิทยานิพนธ์นี้เป็นส่วนหนึ่งของการศึกษาตามหลักสูตรปริญญาวิศวกรรมศาสตรมหาบัณฑิต
สาขาวิชาวิศวกรรมเคมี ภาควิชาวิศวกรรมเคมี
คณะวิศวกรรมศาสตร์ จุฬาลงกรณ์มหาวิทยาลัย
ปีการศึกษา 2565
ลิขสิทธิ์ของจุฬาลงกรณ์มหาวิทยาลัย

Thesis Title	EFFECTS OF ZINC OXIDE ON THERMAL, MECHANICAL, MORPHOLOGICAL, AND GAS BARRIER PROPERTIES OF POLYBUTYLENE SUCCINATE/ POLY(3-HYDROXYBUTYRATE- CO-4-HYDROXYBUTYRATE) FILMS
By	Miss Sunisa Suwatthi
Field of Study	Chemical Engineering
Thesis Advisor	Professor ANONGNAT SOMWANGTHANAROJ, Ph.D.

Accepted by the FACULTY OF ENGINEERING, Chulalongkorn University in
Partial Fulfillment of the Requirement for the Master of Engineering

..... Dean of the FACULTY OF
ENGINEERING
(Professor SUPOT TEACHAVORASINSKUN, D.Eng.)

THESIS COMMITTEE

..... Chairman
(Professor SARAWUT RIMDUSIT, Ph.D.)

..... Thesis Advisor
(Professor ANONGNAT SOMWANGTHANAROJ, Ph.D.)

..... Examiner
(Professor SUTTICHAJ ASSABUMRUNGRAT, Ph.D.)

..... External Examiner
(Assistant Professor Wanchai Lerdwijitjarud, Ph.D.)

สุนิสา สุวัตถิ : ผลกระทบของซิงค์ออกไซด์ที่มีผลต่อคุณสมบัติทางความร้อน ทางกล ทาง
 สัณฐานวิทยา และการต้านทานการซึมผ่านของก๊าซ ของฟิล์มพอลิเมอร์ผสมระหว่างพอลิ
 บิวทิลีนซัคซิเนต และพอลิ(3-ไฮดรอกซีบิวทิเรต-โค-4-ไฮดรอกซีบิวทิเรต). (

EFFECTS OF ZINC OXIDE ON THERMAL, MECHANICAL, MORPHOLOGICAL,
 AND GAS BARRIER PROPERTIES OF POLYBUTYLENE SUCCINATE/ POLY(3-
 HYDROXYBUTYRATE-CO-4-HYDROXYBUTYRATE) FILMS) อ.ที่ปรึกษาหลัก : ศ.

ดร.อนงค์นาฏ สมหวังธนโรจน์

ในปัจจุบันพอลิเมอร์จากปิโตรเคมีมักย่อยสลายได้ยาก และสามารถคงอยู่ในสิ่งแวดล้อม
 เป็นเวลาหลายร้อยปี ปัญหาเหล่านี้จึงส่งผลกระทบต่อ และสร้างมลพิษให้กับสิ่งแวดล้อม ในงานวิจัยนี้
 จึงมีวัตถุประสงค์เพื่อปรับปรุงคุณสมบัติของพอลิเมอร์ชีวภาพที่สามารถย่อยสลายได้ เช่น พอลิบิวทิ
 ลีนซัคซิเนต (PBS) และพอลิ (3-ไฮดรอกซีบิวทิเรต-โค-4-ไฮดรอกซีบิวทิเรต) (P3HB4HB) โดยทำ
 การเลือก P3HB4HB ผสมกับ PBS ในอัตราส่วนต่อน้ำหนักของ PBS:P3HB4HB เท่ากับ 90:10
 และเลือกอนุภาคนาโนซิงค์ออกไซด์เติมลงไปเพื่อเป็นสารก่อให้เกิดผลึกโดยเติมในปริมาณ 0.5, 1
 และ 2% โดยน้ำหนัก โดยกระบวนการผสมจะใช้เครื่องบดผสมระบบปิด และขึ้นรูปเป็นฟิล์มโดย
 กระบวนการขึ้นรูปแบบกดอัด โดยฟิล์มทั้งหมดจะทำการศึกษาโครงสร้างทางเคมี สมบัติทาง
 สัณฐานวิทยา สมบัติทางความร้อน สมบัติทางกลไดนามิก สมบัติทางกล และสมบัติการต้านทาน
 การซึมผ่านของก๊าซ จากผลการวิจัยพบว่าอนุภาคนาโนซิงค์ออกไซด์สามารถปรับปรุงคุณสมบัติ
 ความเป็นผลึก คุณสมบัติทางกล และสมบัติการต้านทานการซึมผ่านของก๊าซ ของพอลิเมอร์ผสม
 ระหว่างพอลิบิวทิลีนซัคซิเนต และพอลิ(3-ไฮดรอกซีบิวทิเรต-โค-4-ไฮดรอกซีบิวทิเรต) ได้

CHULALONGKORN UNIVERSITY

สาขาวิชา วิศวกรรมเคมี

ปีการศึกษา 2565

ลายมือชื่อนิสิต

ลายมือชื่อ อ.ที่ปรึกษาหลัก

6470097021 : MAJOR CHEMICAL ENGINEERING

KEYWORD: polybutylene succinate; poly(3-hydroxybutyrate-co-4-hydroxybutyrate); ZnO nanoparticles; film

Sunisa Suwatthi : EFFECTS OF ZINC OXIDE ON THERMAL, MECHANICAL, MORPHOLOGICAL, AND GAS BARRIER PROPERTIES OF POLYBUTYLENE SUCCINATE/ POLY(3-HYDROXYBUTYRATE-CO-4-HYDROXYBUTYRATE) FILMS. Advisor: Prof. ANONGNAT SOMWANGTHANAROJ, Ph.D.

Currently, conventional polymers from petrochemical processes have low biodegradability and remain in the environment for several hundred years. This has negative effects on the environment. This research aims to improve the properties of biopolymers such as poly(butylene succinate) (PBS) and poly(3-hydroxybutyrate-co-4-hydroxybutyrate) (P3HB4HB). P3HB4HB was selected to blend with PBS in with weight ratios of PBS:P3HB4HB was 90/10 and ZnO nanoparticles (0.5, 1 and 2%) was selected as a nucleating agent. The melt blending process using an internal mixer and molded into a film using a compression molding process. The chemical structures, morphological properties, thermal properties, dynamic mechanical properties, mechanical properties and gas barrier properties of all polymer blend films were evaluated. The results showed that ZnO nanoparticles improved the degree of crystallinity, mechanical, and gas barrier properties of PBS/P3HB4HB blend.

Field of Study: Chemical Engineering

Student's Signature

Academic Year: 2022

Advisor's Signature

ACKNOWLEDGEMENTS

I would like to express my sincere thanks to my advisor, Professor Anongnat Somwangthanaroj, for her help, valuable advice, and continuous support throughout my Master's Degree study and this research.

I would also like to express my sincere thanks to everyone in the Polymer Engineering Research Laboratory for their advice, suggestions, assistance, discussion, friendly encouragement, and guidance through the solving of various problems.

Finally, I most gratefully acknowledge my family for all their support throughout the period of this research.

Sunisa Suwatthi



TABLE OF CONTENTS

	Page
.....	iii
ABSTRACT (THAI).....	iii
.....	iv
ABSTRACT (ENGLISH).....	iv
ACKNOWLEDGEMENTS.....	v
TABLE OF CONTENTS.....	vi
LIST OF TABLES.....	viii
LIST OF FIGURES.....	ix
CHAPTER 1 Introduction.....	1
1.1 Introduction.....	1
1.2 Objectives.....	2
1.3 Scope of research.....	2
CHAPTER 2 Literature reviews.....	3
2.1 Overview.....	3
2.2 Effect of blending on thermal properties.....	5
2.3 Effect of blending on mechanical properties.....	9
2.4 Effect of blending on morphological properties.....	12
2.5 Effect of blending on barrier properties.....	17
2.6 Effect of ZnO on properties of polymer blends.....	18
CHAPTER 3 Experiments.....	22
3.1 Materials.....	22

3.2 Film preparation	22
3.3 Film Characterizations	23
3.3.1 The chemical structure.....	23
3.3.2 Morphological properties	23
3.3.4 Dynamic mechanical properties	23
3.3.5 Mechanical properties	24
3.3.6 Gas barrier properties.....	24
CHAPTER 4 Results and Discussion	25
4. Characterizations of polymer films.....	25
4.1 The Chemical Structures of polymer films.....	25
4.2 Morphological properties	27
4.2.1 Morphology of polymer films	27
4.2.2 The spherulite morphology of all polymer films	28
4.3 Thermal properties of polymer films	30
4.4 Dynamic Mechanical properties.....	32
4.5 Mechanical properties of polymer films.....	34
4.6 Gas barrier properties of polymer films	36
CHAPTER 5 Conclusions	38
Recommendation	38
REFERENCES	39
VITA.....	43

LIST OF TABLES

	Page
Table 2.1 Thermal and mechanical properties of polymers [9, 6, 11, 22, 2, 13].....	3
Table 2.2 Thermal properties of PVC/PBS blends [5]	7
Table 2.3 Thermal properties of PHBHHx/P3HB4HB blends [11].....	8
Table 2.4 Thermal properties of PHB/P3HB4HB blends [6]	8
Table 2.5 Mechanical properties of PLA and PLA/PBS blends [7].....	10
Table 2.6 Mechanical properties of PHBHHx/P3HB4HB blends [11]	12
Table 2.7 Crystallization, Melting and Degradation Temperatures of PHBV/ZnO Nanocomposites [12]	19
Table 2.8 Effect of ZnO on melting temperature and crystallinity (%) of PET/PBS blends	20
Table 2.9 Tensile properties of PET/PBS blends with ZnO (1% and 2%)	21
Table 3.1 Composition of PBS/P3HB4HB/ZnO blends	22
Table 4.1 Thermal properties of all polymer films.	31
Table 4.2 Thermal properties of all polymer films.	32
Table 4.3 Mechanical properties of all polymer films.	34
Table 4.4 Mechanical properties of all polymer films.	36

LIST OF FIGURES

	Page
Figure 2.1 Structure of PBS.....	4
Figure 2.2 Structure of Polyhydroxyalkanoate homo-polymer.....	4
Figure 2.3 Structure of Polyhydroxyalkanoate co-polymer.....	5
Figure 2.4 Structure of Poly(3-hydroxybutyrate-co-4-hydroxybutyrate) or P3HB4HB. ..	5
Figure 2.5 The crystallization of pure PLA (a), PLA/PBS (70/30) blend (b) [7]	6
Figure 2.6 The loss tangent of pure PVC, pure PBS, and PVC/PBS blends [5].....	7
Figure 2.7 Mechanical properties of polymer blends.....	9
Figure 2.8 Mechanical properties of pure PVC, pure PBS and PVC/PBS blends [5].....	11
Figure 2.9 SEM surface (a), SEM cross-section (b) of LLDPE/PBAT, LLDPE/PBS and PBAT/PBS blends	13
Figure 2.10 SEM of cryo-fractured surface of pure PLA, pure PBS, and PLA/PBS blends	14
Figure 2.11 POM of pure PLA (a1), PLA/PBS (70/30) blend (b1), at t=2 min, 119 °C. a2 and b2 at t=30 min, 119 °C [7]	14
Figure 2.12 SEM of pure PVC (a), pure PBS (b), PVC/PBS blends (c–g) (10% (c), 20% (d), 30% (e), 40% (f), and 50% (g) of PBS) [5].....	15
Figure 2.13 SEM of different PHBHHx/P3HB4HB blends without chondrocytes (1 and 2) and with chondrocytes cultured (3)	16
Figure 2.14 Water vapor permeability (WVP) of LLDPE/PBAT, LLDPE/PBS and PBAT/PBS blend films	17
Figure 2.15 Oxygen permeability (OP) of LLDPE/PBAT, LLDPE/PBS and PBAT/PBS blend films.....	18
Figure 2.16 Tensile properties of PHBV/ZnO blends [12].....	19
Figure 2.17 TGA curves of PET/PBS blends with ZnO (1% and 2%).....	20

Figure 4.1 FT-IR spectra of the neat PBS (a) and the neat P3HB4HB (b)	26
Figure 4.2 FT-IR spectra of PBS/P3HB4HB (90/10) blend, PBS/P3HB4HB/ZnO (90/10/0.5), PBS/P3HB4HB/ZnO (90/10/1), and PBS/P3HB4HB/ZnO (90/10/2)	26
Figure 4.3 SEM images from fractured surfaces of the neat PBS (a), the neat P3HB4HB (b), PBS/P3HB4HB (90/10) blend (c), PBS/P3HB4HB/ZnO (90/10/0.5) (d), PBS/P3HB4HB/ZnO (90/10/1) (e), and PBS/P3HB4HB/ZnO (90/10/2) (f).....	28
Figure 4.4 The particles size of ZnO nanoparticles in polymer blend films.....	28
Figure 4.5 POM of the neat PBS at 95°C (a), neat PBS after 5 mins (b).....	29
Figure 4.6 DSC Thermograms of the neat PBS, the neat P3HB4HB and PBS/P3HB4HB (90/10) blends.	30
Figure 4.7 DSC Thermograms of the PBS/P3HB4HB (90/10) blend, PBS/P3HB4HB/ZnO (90/10/0.5), PBS/P3HB4HB/ZnO (90/10/1), and PBS/P3HB4HB/ZnO (90/10/2)	31
Figure 4.8 DMA measurements of the neat PBS, the neat P3HB4HB, PBS/P3HB4HB (90/10) blend (a and b) and PBS/P3HB4HB/ZnO; (a) $\tan\delta$ and (c and d) storage modulus (E') as a function of temperature	34
Figure 4.9 Stress–Strain curves of the neat PBS, the neat P3HB4HB and PBS/P3HB4HB (90/10) blends.	35
Figure 4.10 Stress–Strain curves of the PBS/P3HB4HB (90/10) blend, PBS/P3HB4HB/ZnO (90/10/0.5), PBS/P3HB4HB/ZnO (90/10/1), and PBS/P3HB4HB/ZnO (90/10/2).....	36
Figure 4.11 Oxygen and Water vapor transmission rate of all polymer s films.	37

CHAPTER 1

Introduction

1.1 Introduction

In recent years, bioplastics, including bio-based and biodegradable materials, have been studied and developed as sustainable packaging alternatives to conventional polymers that cause harmful effects on the environment and are difficult to degrade. Biodegradable polymers are environmentally friendly and can be used in a wide range of applications, such as general packaging or food packaging, popular biodegradable polymers including polylactic acid (PLA), poly(butylene adipate-co-terephthalate) (PBAT), and polybutylene succinate (PBS) [7].

Polybutylene succinate (PBS) is an aliphatic polyester that can be chemically synthesized by polycondensing 1,4-butanediol with succinic acid [3]. PBS is a type of biodegradable plastic that is easily obtainable on the market and has exceptional performance characteristics. As a semi-crystalline polymer, PBS can be utilized in a diverse array of applications [9]. Compared to other aliphatic polyesters, PBS has remarkable properties such as high elongation strength, thermal stability, ability to undergo melting process, resistance to chemicals, and biodegradability (it can be composted in compost, moist soil, or seawater) [7, 9]. Despite its exceptional properties, PBS also has some drawbacks, such as a sluggish crystallization rate and low viscosity when melted. Thus, to enhance its application characteristics, PBS needs to be combined with other materials, including fillers and additives [9].

The most recent type of PHAs is Poly(3-hydroxybutyrate-co-4-hydroxybutyrate) (P3HB4HB), which is created through the combination of P3HB and 4-hydroxybutyrate (4HB) monomers during copolymerization. Depending on the molar ratio of 4HB, P3HB4HB can exhibit a wide variety of different morphologies and physical characteristics, range from very crystalline to elastic rubber-like [32, 6].

P3HB4HB has an intriguing feature that can be used for fermentation and degradation processes by microbial activity. P3HB4HB has properties similar to PE and PP and is also able to withstand high temperatures compared with PBS [32, 6, 11].

Zinc oxide (ZnO) nanoparticles have accessibility, affordability, the ability to be surface-modified with various functional groups, and biocompatibility [20]. The addition of ZnO nanoparticles to polymers results in a significant improvement in both the mechanical properties and antibacterial characteristics of the resulting material. [12].

In this study, P3HB4HB was selected to blend with PBS to improve the properties of PBS, and ZnO was selected as a nucleating agent to enhance the thermal, mechanical, morphological, and gas barrier properties of PBS/P3HB4HB blends.

1.2 Objectives

To investigate the effect of ZnO on thermal, mechanical, morphological and gas barrier properties of PBS/P3HB4HB blends.

1.3 Scope of research

1. PBS/P3HB4HB blends with weight ratios of 100/0, 90/10 and 0/100 are mixed.
2. Different weight ratios of PBS/P3HB4HB blends are mixed with ZnO (0.5, 1 and 2 wt%).
3. Thermal, mechanical, morphological and gas barrier properties of PBS/P3HB4HB blends with and without ZnO are studied.

CHAPTER 2

Literature reviews

The effect of types of polymers, polymer blends and addition of additives on the thermal, mechanical, morphological, and barrier properties of polymer blends have been discussed in this chapter.

2.1 Overview

Table 2.1 Thermal and mechanical properties of polymers [9, 6, 11, 22, 2, 13]

Polymer	Glass transition temperature (T_g) (°C)	Crystallization temperature (T_c) (°C)	Melting temperature (T_m) (°C)	Crystallinity (X_c) (%)	Young's modulus (MPa)	Tensile strength (MPa)	Elongation at break (%)
PE	<-90	-	116-132	-	254-924	21.6-24.5	40-617
PP	-4	-	166	-	1729	39.4	140
PBAT	-27.5	63.4	104.6	-	94±5	10.4±1.5	162±13
PCL	-	25.60	60.17	39.3	22.1±1.35	2.47±0.24	149±12.5
PLA	65.33	-	168.53	7.92	2140±55	45±2	13±3
PBS	78	62.2	115	-	561±21	41.8±2.0	27±15
P3HB4HB	-4.3	-	135-160	38.2	543.57±62.41	25.33±1.51	631.31±36.13

Table 2.1. shows the thermal and mechanical properties of polymers. Conventional polymers (for example, PE and PP) have a melting temperature greater than 100 °C, high elongation at break. However, they cannot be decomposed, whereas biodegradable polymers can. PBAT and PCL have low melting temperatures, Young's modulus and tensile strength. PLA has a glass transition temperature of around 60 °C, and is easily deformed when heated. PBS has a melting temperature around 115 °C. P3HB4HB has properties similar to PE and PP and is also able to withstand high temperatures around 135-160 °C [6, 11, 22, 2, 13].

Polybutylene succinate (PBS) is an aliphatic polyester that can be chemically synthesized by polycondensing 1,4-butanediol with succinic acid [3]. The chemical structure of PBS is shown in Figure 2.1. PBS is a high-performing bioplastic that is commercially available. PBS is a versatile semi-crystalline polymer with a semi-crystalline structure [9]. PBS had exceptional characteristics such as high elongation strength, thermal stability, the ability to undergo a melting process, resistance to chemicals, and biodegradability [7, 9]. Despite its exceptional properties, PBS also has some drawbacks, such as a slow crystallization rate and low viscosity when melted. Thus, to enhance its application characteristics, PBS needs to be combined with other materials, including fillers [9].

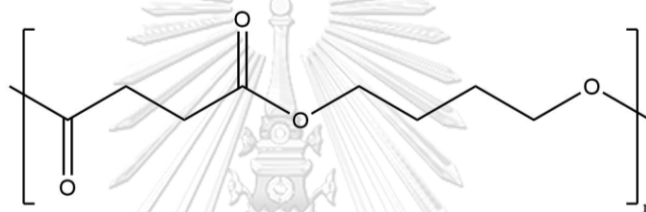


Figure 2.1 Structure of PBS.

Polyhydroxyalkanoates (PHAs) are bio-polyesters produced by microorganisms, they are biodegradable and biocompatibility. [3]. The chemical structure of PHAs is shown in Figure 2.2 and Figure 2.3. PHA materials are highly suitable options for the new generation of environmentally friendly packaging materials. There are over 150 types of PHAs that have been identified, comprising a variety of monomers (depending on the different side chains and lengths of the main chain in the PHA monomer) [11, 2].

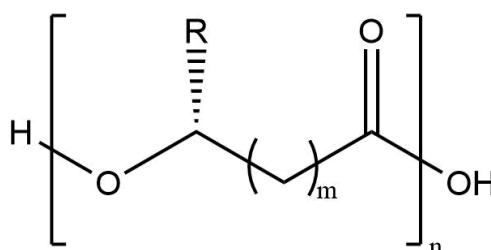


Figure 2.2 Structure of Polyhydroxyalkanoate homo-polymer.

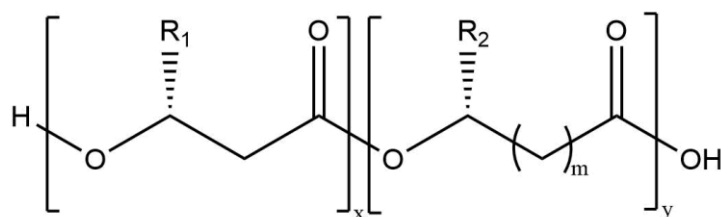


Figure 2.3 Structure of Polyhydroxyalkanoate co-polymer.

The most recent type of PHAs is Poly(3-hydroxybutyrate-co-4-hydroxybutyrate) or P3HB4HB, which is created through the combination of P3HB and 4-hydroxybutyrate (4HB) monomers during copolymerization. The chemical structure of P3HB4HB is shown in Figure 2.4. P3HB4HB has a wide range of physical and morphological properties, depending on the molar percentage of 4HB [32, 6].



Figure 2.4 Structure of Poly(3-hydroxybutyrate-co-4-hydroxybutyrate) or P3HB4HB.

2.2 Effect of blending on thermal properties

Homklin, R. and N. (2013) , showed that the blending of PLA and PBS showed partial miscibility, which was indicated by the decreased T_g of PLA in the blend. The T_g of PLA is found to be reduced in all blends. Due to the difference in their T_{cc} , PBS would initiate crystallization before PLA during the process of cold crystallization. As a result, the crystallization of PLA would be inhibited by the presence of PBS.

Zhang, X., et al. (2021) [19], showed that the crystallization of PLA and PLA/PBS (70/30) was depicted in Figure 2.5. The crystallization peaks of pure PLA were almost the same at different crystallization temperatures, indicating that the variation in temperature had a minor impact on the crystallization of PLA. The PLA/PBS blend was more sensitive to changes in crystallization temperature than

PLA. In comparison to pure PLA, the polymer blend crystallized faster. This indicates that the addition of PBS enhanced the crystallization rate of the PLA.

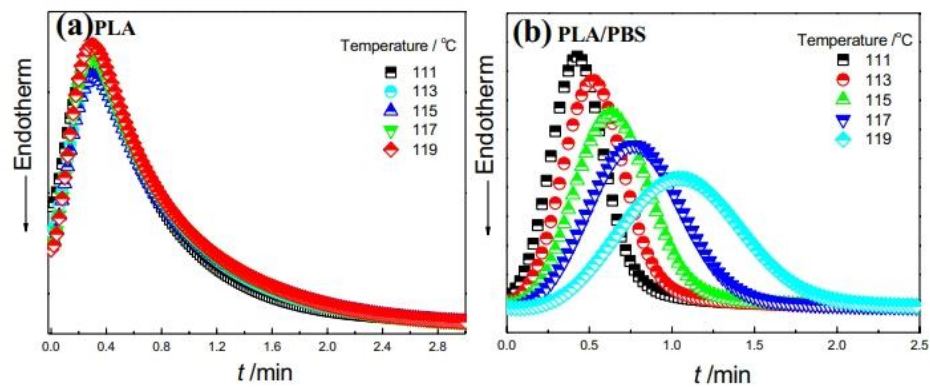


Figure 2.5 The crystallization of pure PLA (a), PLA/PBS (70/30) blend (b) [7]

Chuayjuljit, S., et al. (2019) [20], showed that PVC and PBS had T_g of approximately 100 °C and -10 °C, respectively as shown in figure 2.6 and Table 2.2. Adding PBS to PVC at varying concentrations (10-40%) decrease T_g of PVC constantly as PBS loading increased. This was a result of PBS possessing high flexibility and a low T_g , thus enhancing the mobility of PVC chain. However, at 50% PBS, the T_g of PVC was higher than with low content of PBS. This indicated that the two components had separated in phase. The HDT (Heat deflection temperature) and VST (Vicat softening temperature) of PVC were found to be lower when compared to those of PBS. HDT and VST were reduced when PVC was combined with PBS due to the polymer's increased mobility. Furthermore, the decrease in both HDT and VST of the PVC/PBS blends was caused by the weak interaction between the PVC and PBS interfaces.

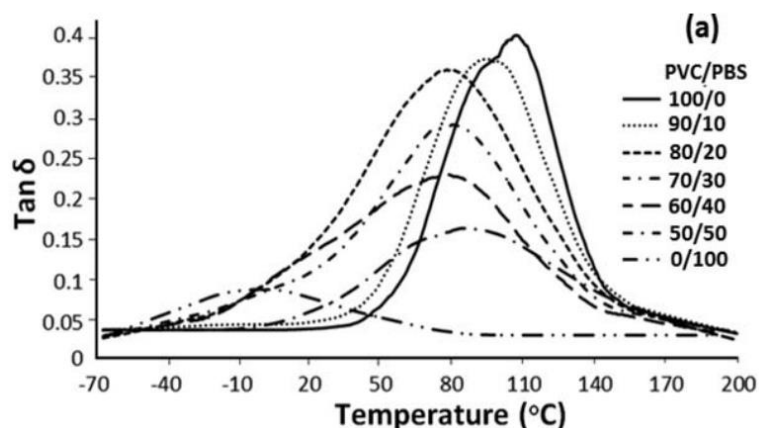


Figure 2.6 The loss tangent of pure PVC, pure PBS, and PVC/PBS blends [5]

Table 2.2 Thermal properties of PVC/PBS blends [5]

Polymer	T_g (°C)	HDT (°C)	VST (°C)
PVC/PBS (100/0)	110	74.8 ± 0.1	69.4 ± 0.3
PVC/PBS (0/100)	-10	99.6 ± 0.1	100.2 ± 0.1
PVC/PBS (90/10)	95	65.3 ± 0.5	55.8 ± 0.3
PVC/PBS (80/20)	80	52.6 ± 0.2	53.5 ± 0.1
PVC/PBS (70/30)	81	52.7 ± 0.2	50.8 ± 0.6
PVC/PBS (60/40)	78	54.8 ± 0.3	49.8 ± 0.1
PVC/PBS (50/50)	85	66.4 ± 0.1	53.5 ± 0.2

Out of all the polymer blends, the PHBHHx/P3HB4HB blend with a weight ratio of 4:2 exhibited the greatest thermal stability as shown in Table 2.3 by the work of Luo, L., X. Wei, and G.Q. Chen [11]. As a result, the PHBHHx/P3HB4HB blends were more thermally stable than PHBHHx. PHBHHx had a T_g of -1.52 °C, but as the concentration of P3HB4HB in the blends increased, there was a corresponding decrease in the T_g of the PHBHHx/P3HB4HB blends.

Table 2.3 Thermal properties of PHBHHx/P3HB4HB blends [11]

Polymer	$T_{d(5\%)} (^\circ\text{C})$	$T_g (^\circ\text{C})$	$T_m (^\circ\text{C})$	$X_c (\%)$
PHBHHx	259.95	-1.52	102.57	25.0
PHBHHx/P3HB4HB (5:1)	278.65	-2.79	122.20	29.9
PHBHHx/P3HB4HB (4:2)	280.54	-2.96	123.11	31.1
PHBHHx/P3HB4HB (3:3)	275.80	-3.67	124.92	32.3
PHBHHx/P3HB4HB (2:4)	272.91	-3.88	125.37	31.3
PHBHHx/P3HB4HB (1:5)	270.51	-3.72	126.99	37.1
P3HB4HB	270.78	-4.30	124.48	38.2

As shown in Table 2.4 by R. Luo et al. (2007) [6], immiscibility between PHB and P3HB4HB was found when P3HB4HB exceeded 50 wt% of the mixture. T_g decreased when P3HB4HB concentration increased in the blends. The lower temperature corresponds to the P3HB4HB phase, whereas the higher temperature corresponds to the PHB phase. When the two polymers were blended, the degradation process was observed to occur in a single, step-by-step manner. As the concentration of P3HB4HB increased from 0 to 50%, there was a slight rise in $T_{d(5\%)}$ (Thermal degradation temperature at 5% weight loss)

Table 2.4 Thermal properties of PHB/P3HB4HB blends [6]

Polymer	$T_g (^\circ\text{C})$	$T_{d(5\%)} (^\circ\text{C})$
PHB/P3HB4HB (100/0)	0.5	235.0
PHB/P3HB4HB (90/10)	-1.0	236.8
PHB/P3HB4HB (80/20)	-2.6	237.7
PHB/P3HB4HB (70/30)	-5.3	240.3
PHB/P3HB4HB (60/40)	-9.0	239.4
PHB/P3HB4HB (50/50)	-9.8	241.3
PHB/P3HB4HB (40/60)	-17.0 and -1.0	246.3
PHB/P3HB4HB (0/100)	-17.7	254.3

2.3 Effect of blending on mechanical properties

Bumbudsanpharoke, N., et al. (2022) , showed in **Figure 2.7** that PBS concentration increased tensile strength proportionally to the LLDPE/PBS and PBAT/PBS blending ratios. Because of the increased compatibility between PBAT and PBS blends, the high tensile strength was maintained. PBS demonstrated lower elongation at break than LLDPE and PBAT. PBAT/PBS blends showed intermediate elongation at break between the neat films, indicating that the elongation at break was corresponding to the components. The outcomes indicated that the tensile strength and elongation at break of PBAT/PBS blends varied in accordance with the ratios at which the polymers were mixed. In LLDPE blends, incompatibilities and nonhomogeneous occurred.

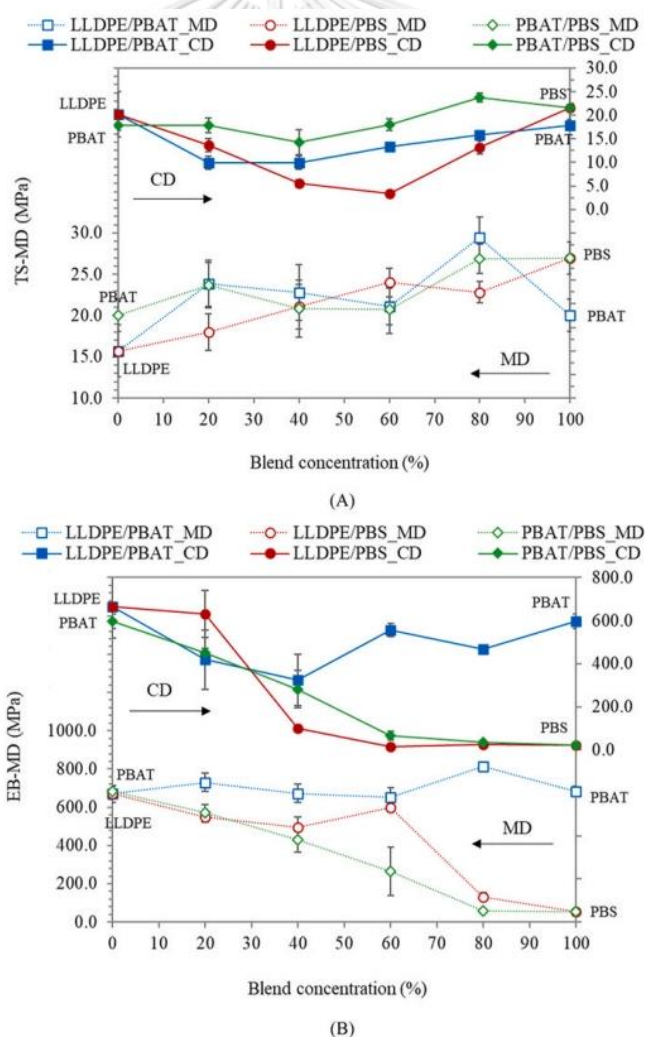


Figure 2.7 Mechanical properties of polymer blends
Tensile strength (TS) (a) and Elongation at break (EB) (b)

Homklin, R. and N. (2013) [18], showed that PLA/PBS blends with a co-continuous structure displayed similar elongation at break values across all ratios, but the tensile strength varied. At 40% PLA blends, tensile strength was similar to that of pure PBS, showing low interfacial bonding between phases despite their partial miscibility. Due to the stiffness of the PLA, increasing the content up to 60% increased the tensile strength.

Zhang, X., et al. (2021) [7], showed in Table 2.5, the elongation at break of PLA was 3%, indicating a hard and brittle tensile property. The elongation at break of the blend enhanced when 30% PBS was added to the PLA, changing the materials from brittle to ductile.

Table 2.5 Mechanical properties of PLA and PLA/PBS blends [7]

Polymer	Young's modulus (MPa)	Tensile strength (MPa)	Elongation at break (%)	Flexural strength (MPa)	Impact strength (MPa)
PLA/PBS (100/0)	718	60.4	3.0	95.3	87
PLA/PBS (0/100)	550	31.0	660	22.8	254
PLA/PBS (70/30)	639	48.4	169	72.0	167

Chuayjuljit, S., et al. (2019) [5], showed that PVC was a hard and brittle plastic due to its extremely low impact strength, as shown in Figure 2.8. All of the blends had an impact strength that was higher than PVC. Results indicated that the flexibility of PBS reduced the brittleness. The blend that consisted of 20% PBS exhibited a significantly higher impact strength compared to the pure PVC. This could be attributed to enhanced PBS dispersion and stress transfer. When PBS was added in higher amounts (30–50%), the compatibility of the blend was reduced, which led to a decline in impact strength. Moreover, the tensile strength of PVC/PBS blends was inferior to that of pure PVC and decreased as the proportion of PBS in the blend was

raised. This is because PBS has a low inherent tensile strength and flexibility. Additionally, since PBS has a low modulus and is inherently flexible, the stiffness of the PVC/PBS blends decreased as the amount of PBS increased, which resulted in a decrease in the tensile modulus of the PVC. Maximum elongation at break was reached for the PVC/PBS (80/20) blend. This could also be attributed to the flexibility of PBS, which improved the mobility of PVC chains.

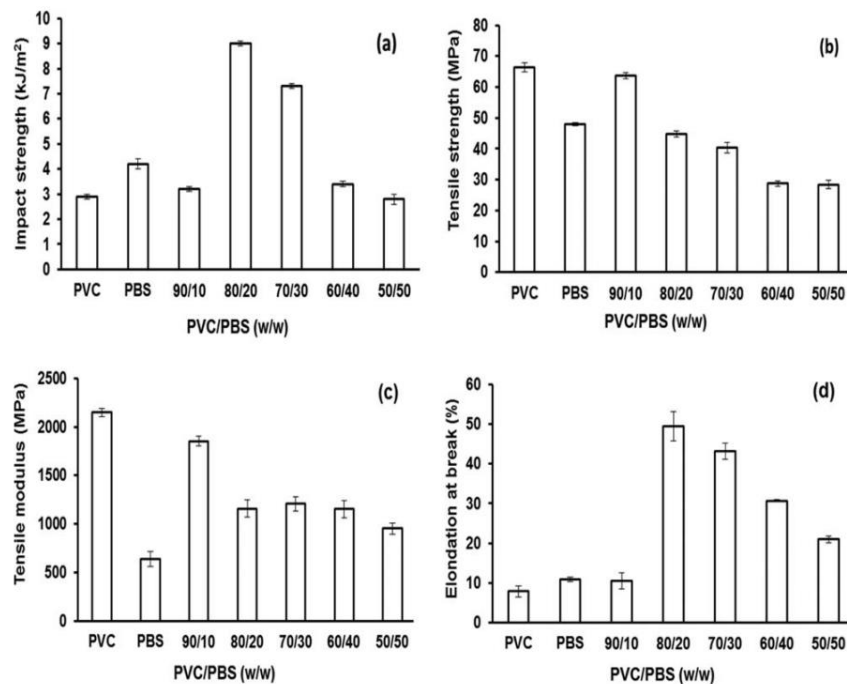


Figure 2.8 Mechanical properties of pure PVC, pure PBS and PVC/PBS blends [5]
 impact strength (a), tensile strength (b), tensile modulus (c), and elongation at break (d)

Luo, L., X. Wei, and G.Q. Chen. (2009) [11], showed in Table 2.6 that compared to PHBHHx, all PHBHHx/P3HB4HB blends exhibited increased elongation at break, with the 3:3 weight ratio having the highest value. This suggests that the blends were more flexible than PHBHHx. As the P3HB4HB content increased, the tensile strength of all the blends also increased. Most of the blends and PHBHHx did not significantly differ from one another in terms of Young's modulus.

R. Luo et al. (2007) [6], showed that the blend of PHB/P3HB4HB demonstrated higher toughness and thermal stability than neat PHB. Therefore,

PHBHHx/P3HB4HB (50/50) represented the solubility limit of blends. In addition, Young's modulus, tensile strength, and stress at break of blends are decreased with increasing P3HB4HB content.

Table 2.6 Mechanical properties of PHBHHx/P3HB4HB blends [11]

Polymer	Tensile strength (MPa)	Young's modulus (MPa)	Elongation at break (%)
PHBHHx	10.14 ± 1.10	496.24 ± 2.21	129.57 ± 23.55
PHBHHx/P3HB4HB (5:1)	15.1 ± 1.31	419.74 ± 36.36	572.97 ± 141.40
PHBHHx/P3HB4HB (4:2)	17.41 ± 1.66	435.86 ± 76.46	611.03 ± 147.07
PHBHHx/P3HB4HB (3:3)	20.91 ± 1.48	408.51 ± 20.48	785.06 ± 46.17
PHBHHx/P3HB4HB (2:4)	23.20 ± 3.31	479.00 ± 68.50	729.62 ± 127.03
PHBHHx/P3HB4HB (1:5)	21.75 ± 2.78	466.52 ± 20.93	678.70 ± 95.37
P3HB4HB	25.33 ± 1.51	543.57 ± 62.41	631.31 ± 36.13

2.4 Effect of blending on morphological properties

Bumbudsanpharoke, N., et al. (2022) [1], showed in the Figure 2.9 that the surfaces of LLDPE, PBAT, and PBS were smooth. However, when PBAT and PBS were blended into LLDPE, the surface structures became non-smooth and layered, which was more pronounced in 40% LLDPE than in 60% LLDPE. In comparison, PBAT/PBS blends exhibited excellent compatibility (similar structures). Both PBAT and PBS have oxygen atoms with carbonyl and ester functional groups, making them less miscible with LLDPE.

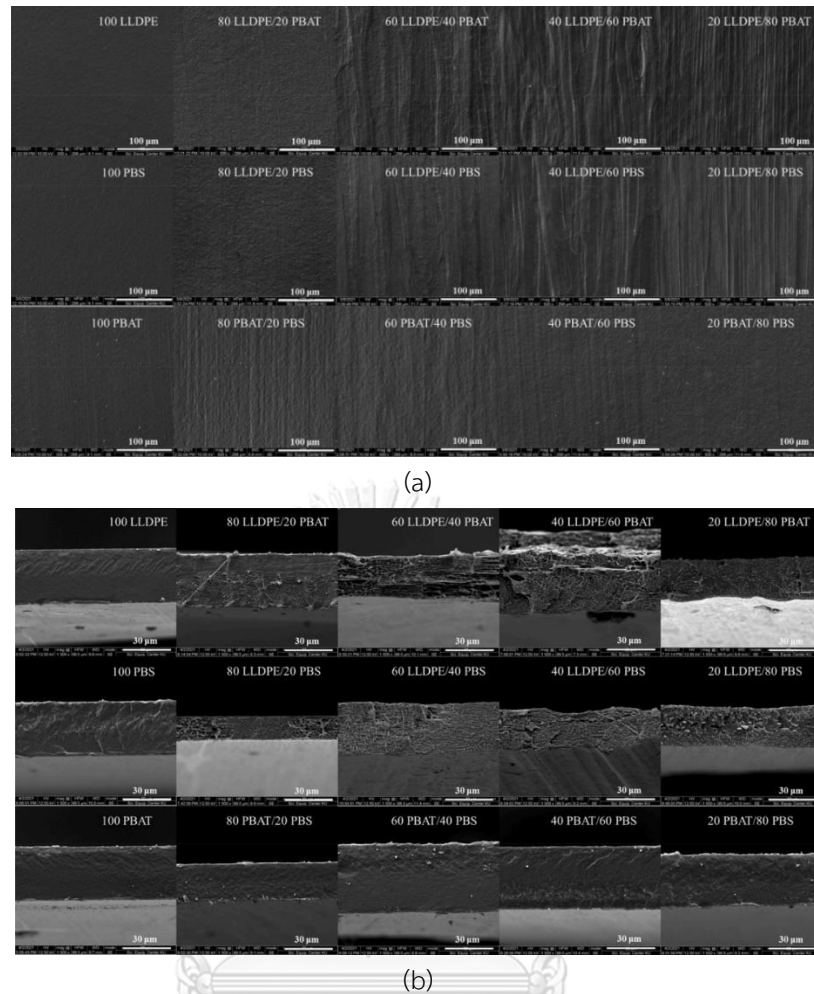


Figure 2.9 SEM surface (a), SEM cross-section (b) of LLDPE/PBAT, LLDPE/PBS and PBAT/PBS blends

From the work of Homklin, R. and N. (2013) [18], Figure 2.10 displays SEM micrographs of cryo-fractured PLA, PBS, and PBS/PLA surfaces. The smoother fracture surface of PLA implies the brittleness of its polymer matrix, whereas PBS displayed a rougher surface and ductile fracture behavior upon being fractured. In the PLA/PBS (50/50) blend, a co-continuous morphology and ductile behavior were observed. However, in the PLA/PBS (40/60) blend, phase inversion occurred, resulting in dispersed phases of PLA droplets. This is because the interfacial bonding between the PLA phases and the PBS phases is not very strong, and the viscosity of the PLA dispersed phases is much higher in the PBS matrix, which has a comparatively lower

viscosity. In contrast, dispersed phases of PBS could not be seen clearly in 60% PLA blends.

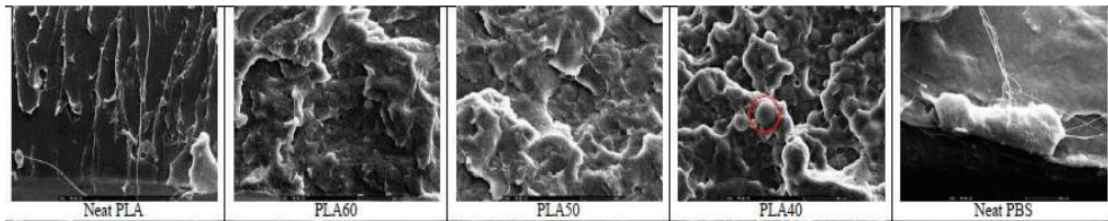


Figure 2.10 SEM of cryo-fractured surface of pure PLA, pure PBS, and PLA/PBS blends

Zhang, X., et al. (2021) [7], showed in Figures 2.11 that at 2 min, there was a notable rise in the number of spherulites in PLA/PBS (70/30) when compared to pure PLA, which suggests that the PBS component could accelerate the crystallization of pure PLA by introducing nuclei. This change in the crystal morphology of the PLA phase will undoubtedly impact the mechanical and other overall properties.

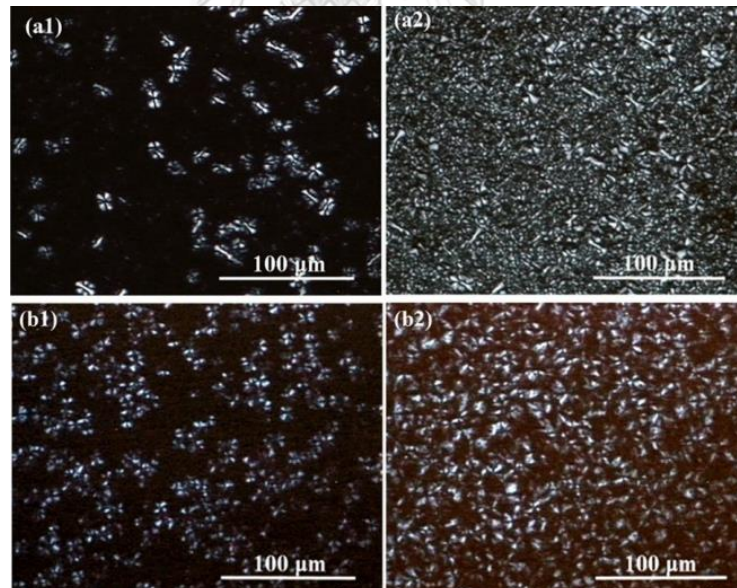


Figure 2.11 POM of pure PLA (a1), PLA/PBS (70/30) blend (b1), at $t=2$ min, 119 °C. a2 and b2 at $t=30$ min, 119 °C [7]

As indicated in the work of Chuayjuljit, S., et al. (2019) [20]. As shown in Figure 2.12, the fractured surface of PVC exhibited cracks, which is a sign of brittleness, while the fractured surface of PBS showed signs of ductility. The PVC/PBS blends had

much rougher fractured surfaces, which showed that the blends had become more ductile, especially the PVC/PBS blend with a composition of PVC/PBS (80/20) blend, which had the highest impact strength and elongation at break. Due to the high flexibility of PBS, PVC/PBS blends were strengthened. In addition, SEM images of PVC/PBS blends with 40-50% PBS exhibited a rough cracked surface with big holes and cavities as a result of the incompatibility between the two materials and their phase separation, as a result, their mechanical properties deteriorated.

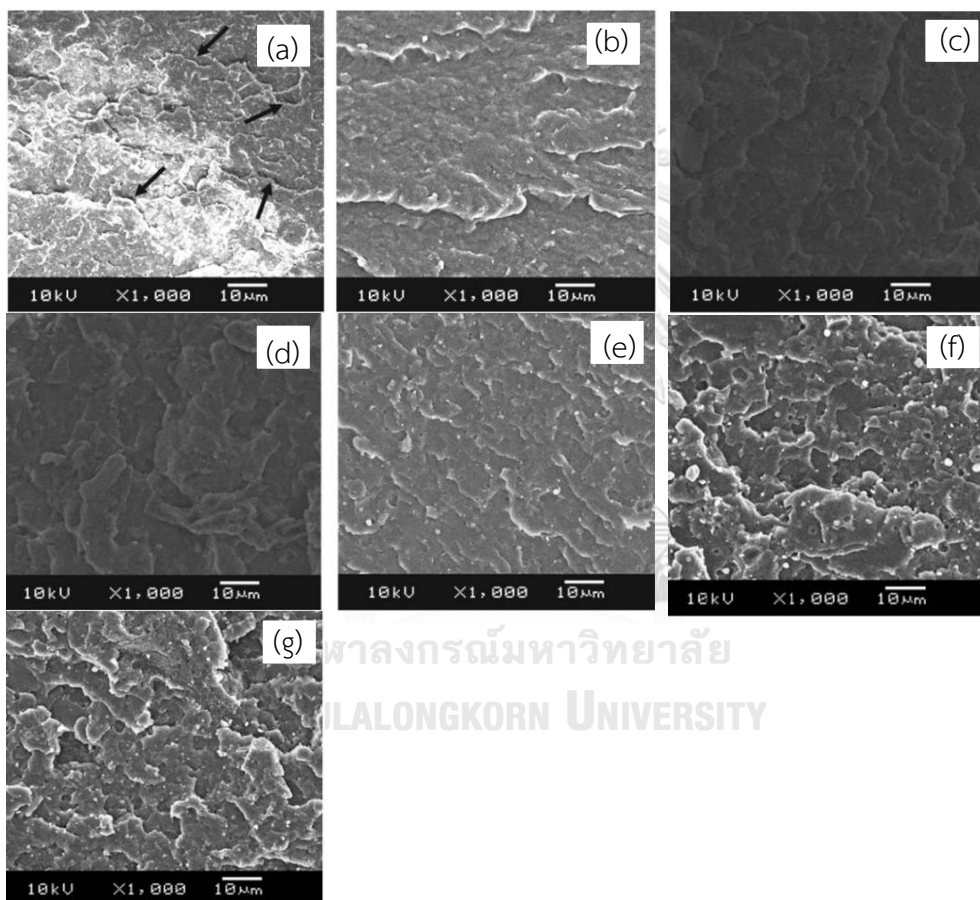


Figure 2.12 SEM of pure PVC (a), pure PBS (b), PVC/PBS blends (c–g) (10% (c), 20% (d), 30% (e), 40% (f), and 50% (g) of PBS) [5]

Luo, L., X. Wei, and G.Q. Chen. (2009) [7], showed that all of the films had a rough surface, but the morphologies of the various films were obviously differentiated as shown in Figure 2.13. Both PHBHHx and PHBHHx/P3HB4HB blended at a weight ratio of 5:1 had raised areas on the surface of their films (Figure. 2.13a2

and 2.13b2). PHBHHx film protuberances had smooth surfaces (Figure 2.13a2). In comparison, the protuberances on the blends with a weight ratio of 5:1 had a rough exterior (Figure 2.13b2). The surface of the film made from blends with a weight ratio of 4:2 had pores that were of varying sizes (Figure 2.13c2).

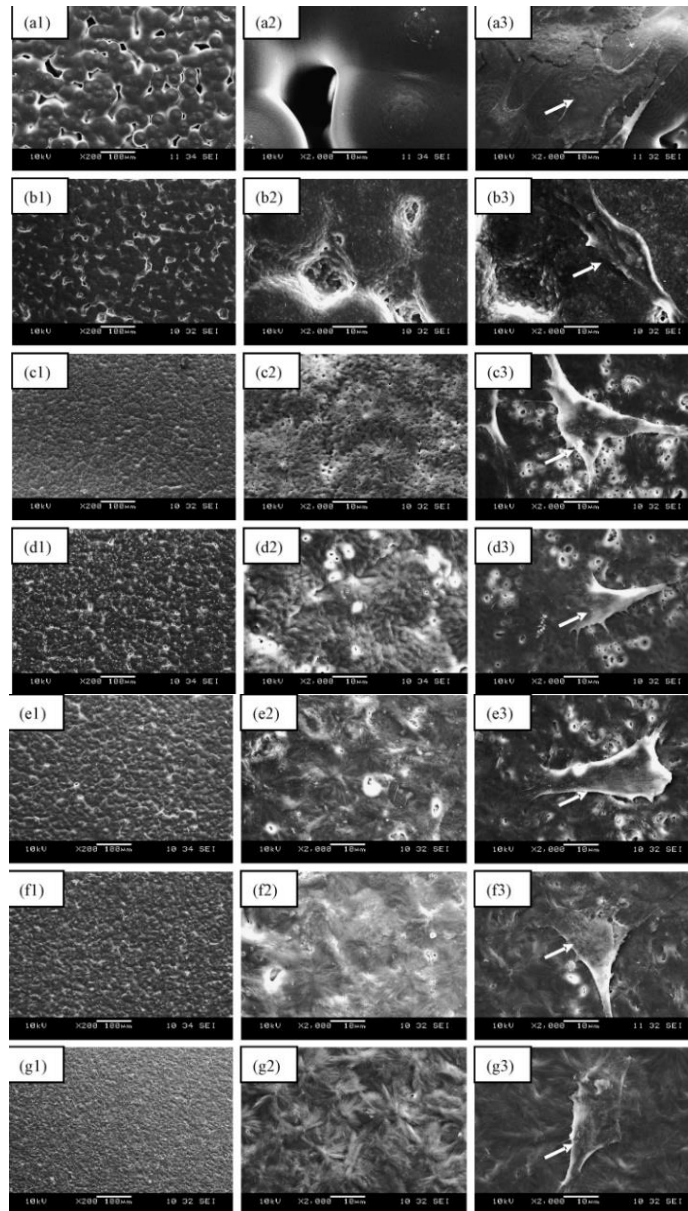


Figure 2.13 SEM of different PHBHHx/P3HB4HB blends without chondrocytes (1 and 2) and with chondrocytes cultured (3)

PHBHHx (a1-a3), 5:1 (b1-b3), 4:2 (c1-c3), 3:3 (d1-d3), 2:4 (e1-e3), 1:5 (f1-f3), P3Hb4HB (g1-g3) [11]

2.5 Effect of blending on barrier properties

Bumbudsanpharoke, N., et al. (2022) , reported that LLDPE showed the lowest WVP owing to the hydrophobic characteristics of hydrocarbon molecules, while PBS exhibited reduced WVP and OP compared to PBAT as a result of its higher crystalline structure. **Figure 2.14** demonstrates that WVP was not impacted by blending PBAT and PBS up to a ratio of 40%. However, as the ratio increased beyond this point, WVP increased, approaching the WVP of PBAT and PBS. PBS content increased, the WVP of PBAT/PBS blend decreased due to an increase in crystallinity. Higher crystallinity led to a reduction in the number of amorphous regions through which permeants were able to diffuse (**Figure 2.14**). As the ratio of PBAT and PBS increased, the OP of LLDPE decreased significantly. The carbonyls and ester bonds of PBAT and PBS increase the hydrophilicity of the matrix, resulting in a lower OP. The PBAT/PBS blend possessed an OP proportional to its polymer components. When the proportion of crystalline PBS was increased in comparison to PBAT, it resulted in a more convoluted path in the amorphous phase, leading to a reduction in oxygen diffusion. (**Figure 2.15**).

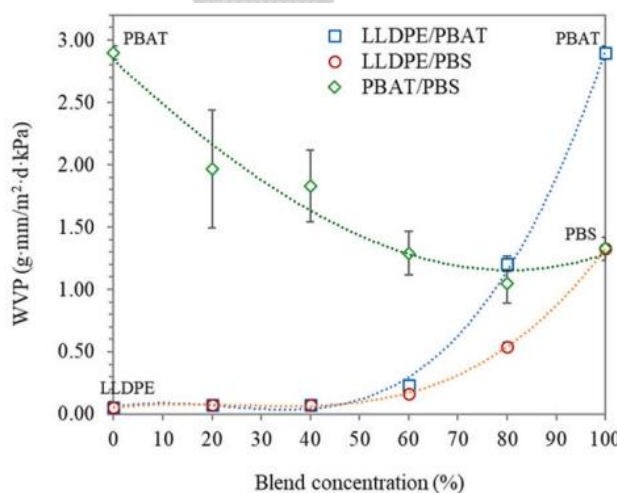


Figure 2.14 Water vapor permeability (WVP) of LLDPE/PBAT, LLDPE/PBS and PBAT/PBS blend films

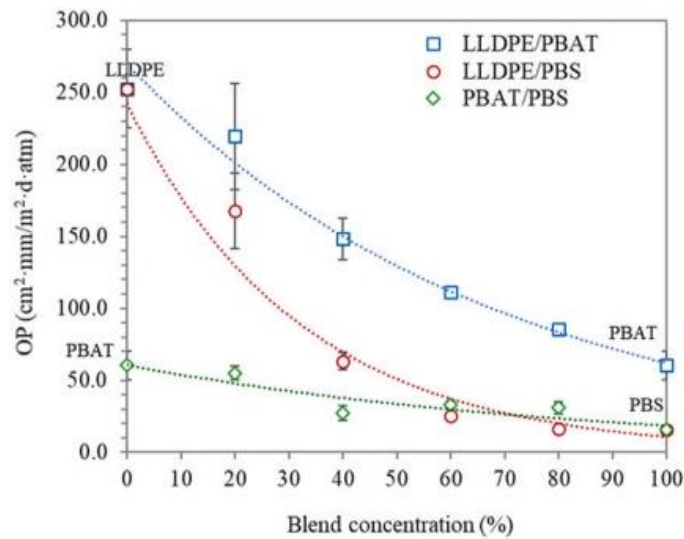


Figure 2.15 Oxygen permeability (OP) of LLDPE/PBAT, LLDPE/PBS and PBAT/PBS blend films

2.6 Effect of ZnO on properties of polymer blends

Diez-Pascual, A.M. and A.L. Diez-Vicente. (2014) [12], reported when PHBV/ZnO is incorporated into bionanocomposites, zinc oxide (ZnO) is an effective reinforcement for improving polymer properties. ZnO increases the crystallization peak temperature and melting temperature, while also increasing the heat resistance of the polymer compound. The crystallinity (X_c) exhibits a significant increase for polymer blends containing 4.0% ZnO, while it decreases at higher concentrations (8.0% ZnO) (Table 2.7). When the filler content exceeded 7%, the reduced crystallinity was caused by the intermingling of polymer chains between the filler and matrix phases, which impeded the movement of the PHBV segments that were crystalline. (Table 2.7).

Several factors can impact the mechanical properties of polymer composites, such as the phase in which the filler is dispersed and the degree of crystallinity in the matrix. As shown in Figure 2.16, the uniform dispersion of the nanofiller, its strong bonding with PHBV, and the higher crystallinity of the matrix resulted in enhanced tensile properties of the polymer.

Table 2.7 Crystallization, Melting and Degradation Temperatures of PHBV/ZnO Nanocomposites [12]

ZnO (wt%)	T_p (°C)	T_m (°C)	X_c (%)	T_{max} (°C)
0	77.3	165/176	55.1	351.3
1.0	86.4	167/177	59.5	363.6
2.0	93.5	168/177	62.8	372.3
4.0	99.1	170/176	66.3	377.0
8.0	103.4	171	63.2	382.9

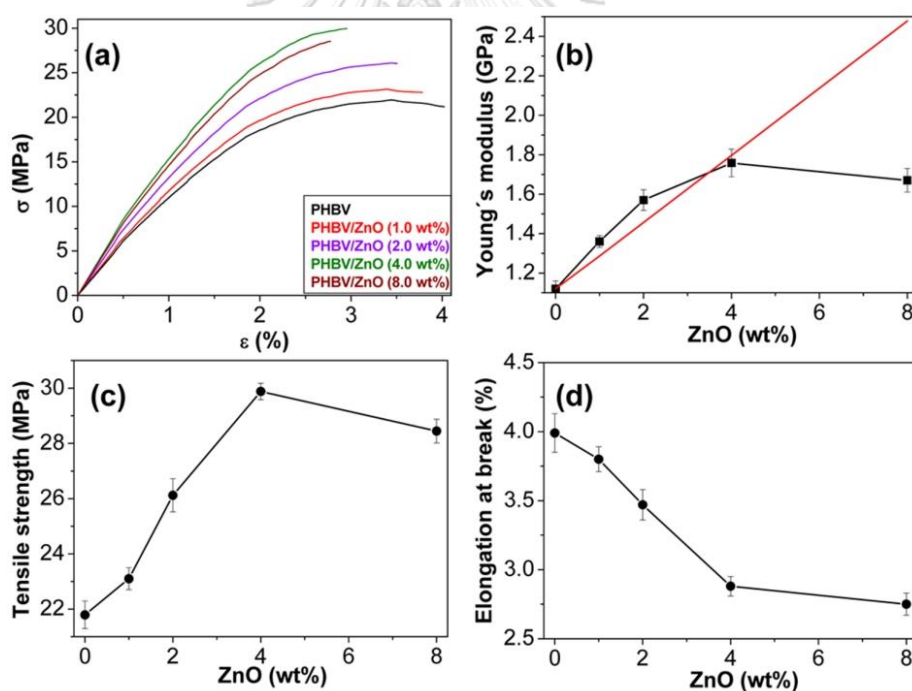


Figure 2.16 Tensile properties of PHBV/ZnO blends [12]

stress-strain curves (a), Young's modulus (b), tensile strength (c) and strain at break (d)

Threepopnatkul, P., et al. (2014) , reported the effect of ZnO on thin film properties, a thin film of a 90:10 PET/PBS blend was chosen. At 1% ZnO addition to the polymer blends, the percentage of crystallinity was higher than PET. When 2%

ZnO was added to PET/PBS blends, the crystallinity of both PET and PBS decreased by a significant amount. Because the high amount of 2% ZnO tended to aggregate commonly. Additionally, the addition of ZnO had no effect on the melting temperature of PET/PBS blends (Table 2.8).

Table 2.8 Effect of ZnO on melting temperature and crystallinity (%) of PET/PBS blends

Filler Content	T_m (°C)		X_c (%)	
	PET	PBS	PET	PBS
0	250	110	7.42	4.19
ZnO 1%	248	106	10.65	2.48
ZnO 2%	247	107	7.47	2.00

TGA testing was carried out on blends of PET/PBS with ZnO at concentrations of 1% and 2% (**Figure 2.17**). PET/PBS blends with 2% ZnO exhibited a lower onset temperature for thermal degradation. The presence of ZnO during the degradation process of PBS, induced by thermal energy, generated free oxygen and oxygen vacancies in the lattice.

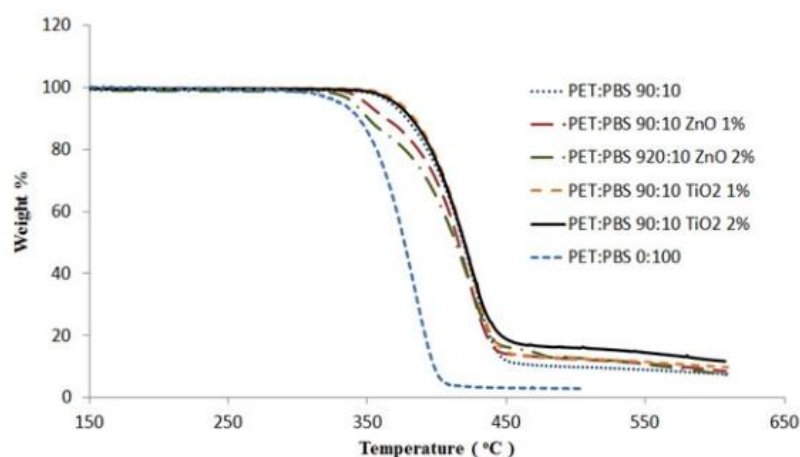


Figure 2.17 TGA curves of PET/PBS blends with ZnO (1% and 2%)

As seen in Table 2.9, the addition of ZnO powder resulted in a small increase in Young's modulus, likely due to the high stiffness of ZnO particles. However, the addition of ZnO did not impact the tensile strength or elongation at break.

Table 2.9 Tensile properties of PET/PBS blends with ZnO (1% and 2%)

Filler Content	Tensile strength (MPa)	Young's modulus (MPa)	Elongation at break (%)
0	27.0 ± 1.6	1820 ± 61	1.78 ± 0.24
ZnO 1%	27.3 ± 2.4	1966 ± 67	1.90 ± 0.28
ZnO 2%	27.6 ± 2.3	1862 ± 96	1.89 ± 0.22



CHAPTER 3

Experiments

3.1 Materials

PBS (BioPBS™ FZ91PM) was purchased from PTT MCC Biochem Company Limited, Thailand. P3HB4HB (EM10080) was obtained from Shenzhen Ecomann Biotechnology Co., Ltd. Zinc Oxide Nanoparticles (ZoNoP®) was obtained from Nano Materials Technology Limited, Thailand.

3.2 Film preparation

The PBS, P3HB4HB and ZnO nanoparticles were dried in an oven at 80 °C, 24 h. to eliminate moisture. The weight ratio for each blending was shown in Table 3.1

Table 3.1 Composition of PBS/P3HB4HB/ZnO blends

Polymer	Content of PBS (phr)	Content of P3HB4HB (phr)	Content of ZnO (phr)
PBS/P3HB4HB/ZnO (100/0/0)	100	0	0
PBS/P3HB4HB/ZnO (0/100/0)	0	100	0
PBS/P3HB4HB/ZnO (90/10/0)	90	10	0
PBS/P3HB4HB/ZnO (90/10/0.5)	90	10	0.5
PBS/P3HB4HB/ZnO (90/10/1.0)	90	10	1
PBS/P3HB4HB/ZnO (90/10/2.0)	90	10	2

The melt blending process for all polymer films was prepared by using an internal mixer. The mixing speed was 50 rpm, and the temperature was 160 °C, mixing time of 5 minutes, and then cut into the pellet. After blending, the compound pellets were molded into a film using a compression molding machine. The compressing temperature was 160 °C for 5 minutes (pre-heated for 5 minutes and cooled with water for 15 minutes). Thickness of polymer blend films was 150-200 μm.

3.3 Film Characterizations

3.3.1 The chemical structure

The chemical structures of all polymer films were analyzed by using Fourier transform infrared spectroscopy (FT-IR) (Nicolet iS5 FT-IR spectrometer with iD7 ATR accessory (Thermo Fisher Scientific Inc., Waltham, MA, USA). All spectral acquisitions were taken with 32 scans at a resolution of 4 cm^{-1} and wavenumber ranging from 4000 to 650 cm^{-1}

3.3.2 Morphological properties

Morphology of the distribution of all polymer films were carried out by using a scanning electron microscope (SEM) (FEI, QuantaTM 250 FEG-SEM) at an accelerating voltage of 10 kV. The polymer blend films were cryogenically fractured in liquid nitrogen and coated with gold.

The spherulite morphology of all polymer blend films were carried out by using a polarizing optical microscope (POM) (DMRXP, LEICA). All of the polymer blend films were heated from 25 to $160\text{ }^{\circ}\text{C}$ at a rate $20\text{ }^{\circ}\text{C}/\text{min}$ and maintain the temperature for 5 min to eliminate the heat history. Then the polymer films were cooled to $95\text{ }^{\circ}\text{C}$ at a rate $1\text{ }^{\circ}\text{C}/\text{min}$ and held isothermally.

3.3.3 Thermal properties

Thermal analysis was performed by using a differential scanning calorimeter (DSC) (Model DSC1, Mettler-Toledo, Switzerland). All of the polymer blend films (5 mg) were heated from -60 to $200\text{ }^{\circ}\text{C}$, held isothermally for 2 min, and then cooled to $-60\text{ }^{\circ}\text{C}$ at a rate of $10\text{ }^{\circ}\text{C}/\text{min}$ (run 2 steps to eliminate the heat history). For all measurements, nitrogen gas was used at a flow rate of $50\text{ mL}/\text{min}$.

3.3.4 Dynamic mechanical properties

Dynamic mechanical analysis was performed by using a dynamic mechanical analyzer (DMA) (model DMA1, Mettler-Toledo, Switzerland). All of the polymer blend films were carried out at a frequency of 1 Hz, and a heating rate of $3\text{ }^{\circ}\text{C}/\text{min}$ from $-60\text{ }^{\circ}\text{C}$ to $80\text{ }^{\circ}\text{C}$ under atmospheric air. All of the polymer blend films were cut into rectangular shapes with a 5 mm width and a 10 mm length.

3.3.5 Mechanical properties

Tensile strength and percentage of elongation at break were measured by using the Universal Testing Machine (Instron 5567, NY, USA) according to ASTM D882. All of the polymer blend films were cut into rectangular shapes with a 20 mm width and a 100 mm length. With a 1 kN load cell, the gauge length and grip separation rates are 50 mm and 12.50 mm/min, respectively.

3.3.6 Gas barrier properties

Oxygen transmission rate (OTR) of all polymer blend films was measured by using an oxygen permeation analyzer (OX-TRAN 2/21, Mocon, USA) at 23°C and 0% RH (relative humidity), using a 50 cm³/min oxygen flow rate according to ASTM D3985. The polymer blend films were cut into a circle mold of equipment with a 5 cm² surface area.

Water vapor transmission rate (WVTR) of all polymer films was measured by using a water vapor permeation analyzer (PERMATRAN-W Model 398, Mocon, USA) at 37.8 °C and 90% RH (relative humidity) according to ASTM E-398. The polymer blend films were cut into a circle mold of equipment with a 5 cm² surface area.

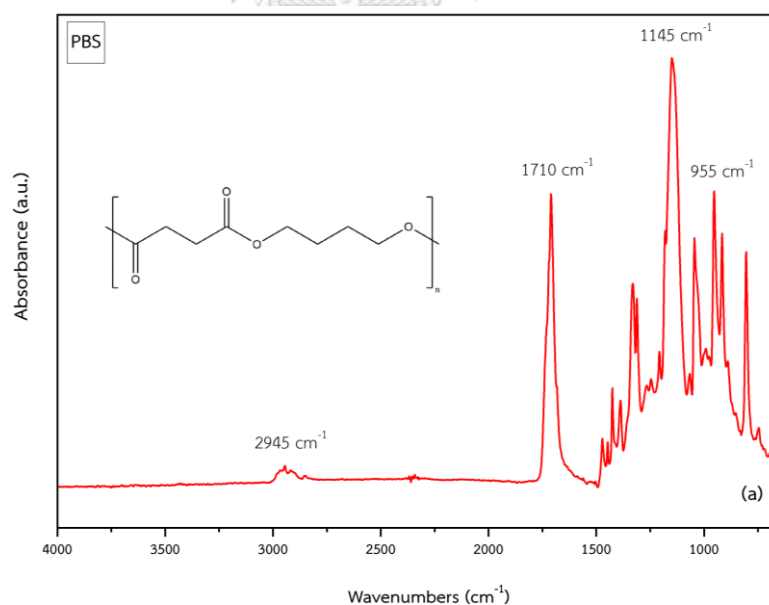
CHAPTER 4

Results and Discussion

4. Characterizations of polymer films

4.1 The Chemical Structures of polymer films

The chemical structures of all polymer films were investigated by Fourier transform infrared spectroscopy (ATR FT-IR). In Figure 4.1(a), the neat PBS had bands at 955 cm^{-1} that correspond to -C-OH bending of carboxylic groups in PBS, 1043 cm^{-1} that correspond to -O-C-C- stretching vibration, 1145 cm^{-1} that correspond to C-O-C in ester groups, 1710 cm^{-1} that correspond to C=O in carbonyl groups and 2945 cm^{-1} that correspond to C-H stretching vibrations [2]. In Figure 4.1(b), the neat P3HB4HB had bands at 871 cm^{-1} were due to C-O-C asymmetric stretching vibrations. The bands at 1015 and 1253 cm^{-1} that correspond to C-O-C , and -CH group, respectively [6]. The bands at 1708 cm^{-1} that correspond to C=O in carbonyl groups.



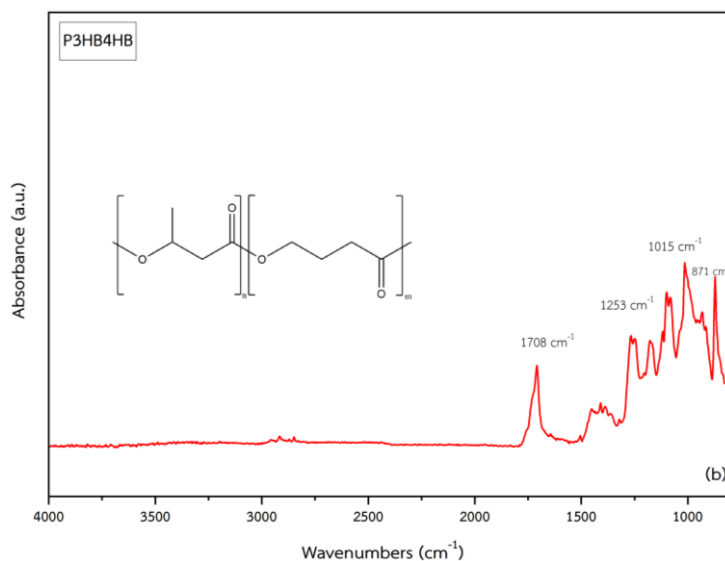


Figure 4.1 FT-IR spectra of the neat PBS (a) and the neat P3HB4HB (b)

The spectrum of polymer blend films with ZnO nanoparticles is shown in Figure 4.2, the new absorption band appeared at 1332 cm^{-1} that correspond to CH_3 vibration. The bands at 3410 cm^{-1} were attributed to hydrogen bonding between ZnO and carbonyl groups ($\text{C}=\text{O}$) in polymer blend films. When ZnO increases, the peak intensity is increased. The reason for this is that the ZnO increased the degree of hydrogen bonding.

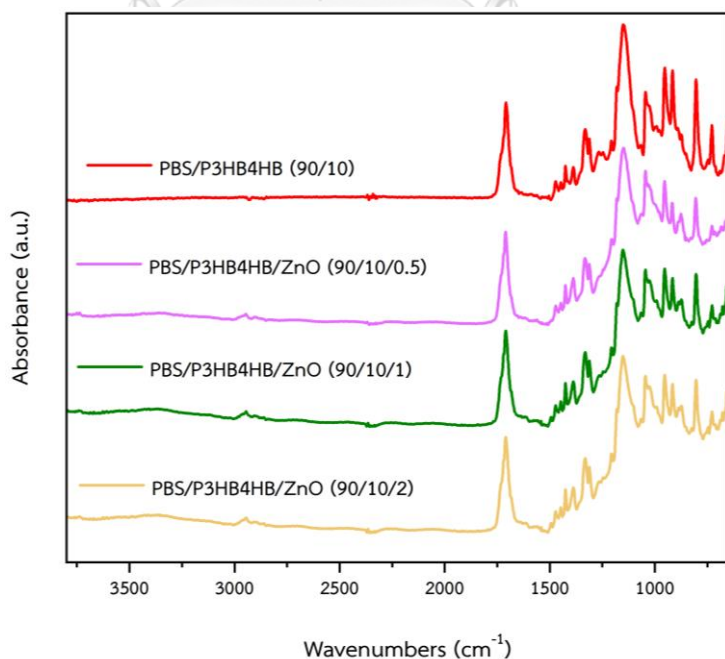
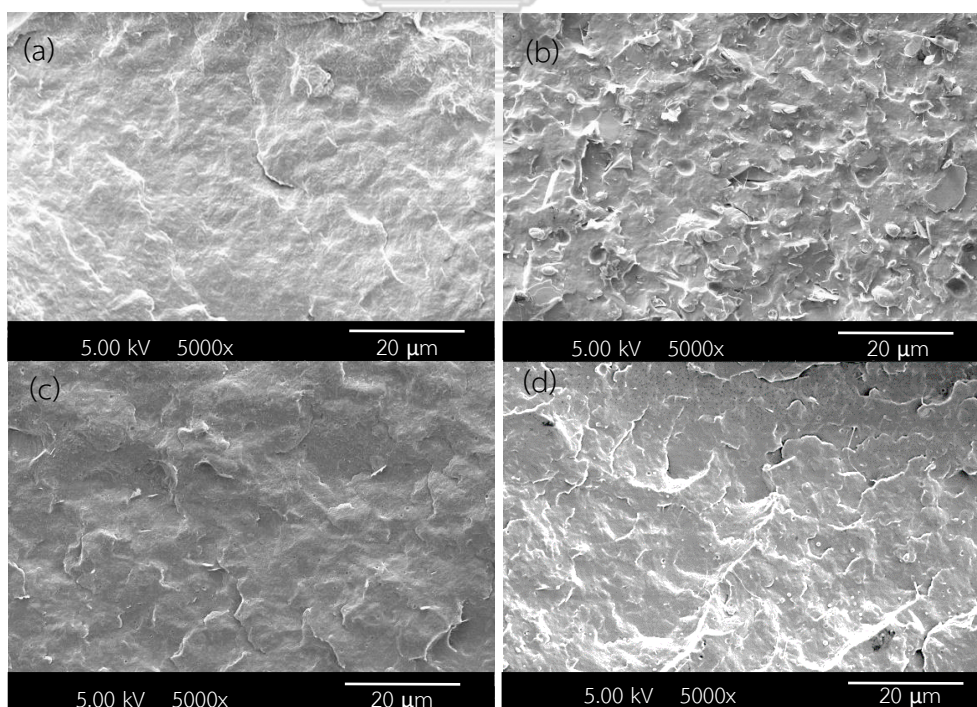


Figure 4.2 FT-IR spectra of PBS/P3HB4HB (90/10) blend, PBS/P3HB4HB/ZnO (90/10/0.5), PBS/P3HB4HB/ZnO (90/10/1), and PBS/P3HB4HB/ZnO (90/10/2)

4.2 Morphological properties

4.2.1 Morphology of polymer films

The morphology of polymer films was studied by using a scanning electron microscope (SEM). As shown in Figure 4.3(a), the neat PBS showed smooth surface and fractured surface [7]. In Figure 4.3(b), the neat P3HB4HB showed a rougher surface than PBS and had some small spherical particles dispersion in the surface [11]. The PBS/P3HB4HB (90/10) blend showed heterogenous phases between PBS and P3HB4HB. The PBS/P3HB4HB (90/10) blend had small spherical particles droplets of P3HB4HB dispersed in the PBS phases. Figure 4.3(d-f), showed small particles of ZnO nanoparticles dispersed in polymer films [20]. As can be seen in Figure 4.4, when adding ZnO nanoparticles (0.5, 1, and 2 wt%), the particle size of ZnO nanoparticles increased from 97.0 to 807.8 nm. The reason for this is that the ZnO nanoparticles were agglomerated their influence on the surface, the surface became rough when the addition of ZnO nanoparticles was added due to the particles agglomerating.



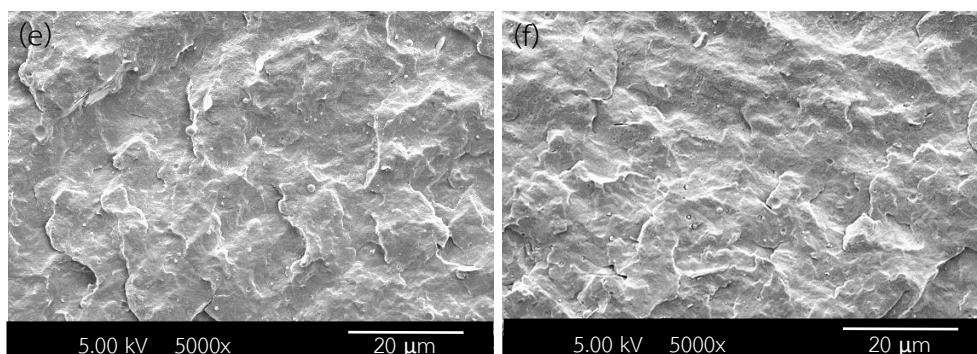


Figure 4.3 SEM images from fractured surfaces of the neat PBS (a), the neat P3HB4HB (b), PBS/P3HB4HB (90/10) blend (c), PBS/P3HB4HB/ZnO (90/10/0.5) (d), PBS/P3HB4HB/ZnO (90/10/1) (e), and PBS/P3HB4HB/ZnO (90/10/2) (f)

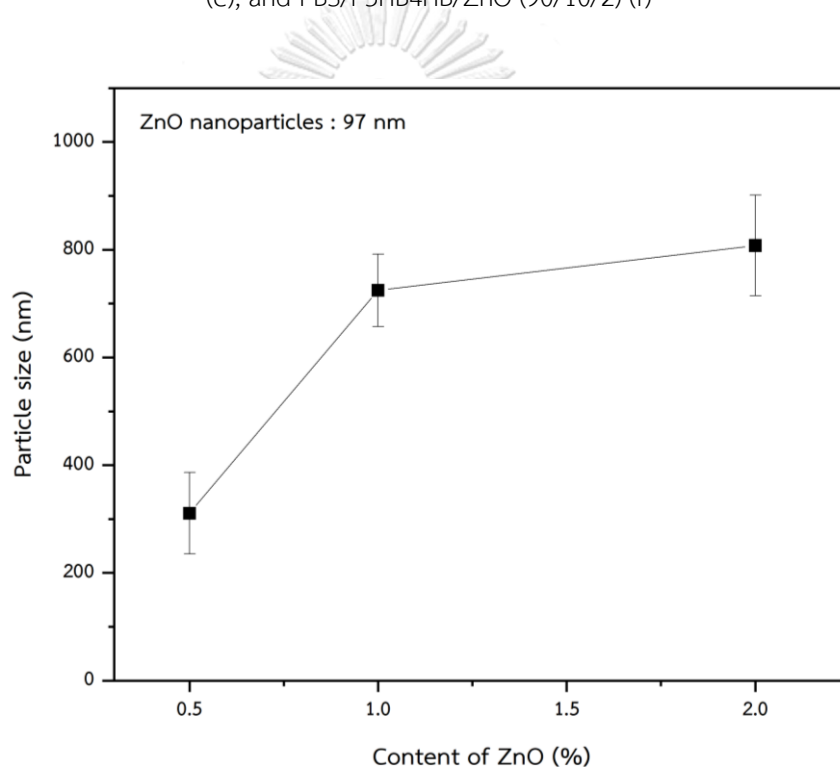


Figure 4.4 The particles size of ZnO nanoparticles in polymer blend films

4.2.2 The spherulite morphology of all polymer films

The spherulite morphology of all polymer films was carried out by using a polarizing optical microscope (POM). All polymer blends were heated to 160 °C heating rate of 20 °C/min and then cooled to 95 °C cooling rate of 1 °C/min. As shown in Figure 4.5(a), nucleating site which is the crystallization of the neat PBS can be observed starting around 95 °C, and after 5 mins the spherulites formed very fast and become more intensive to filled whole area in Figure 4.5(b) [2]. As shown in

Figure 4.5(c), nucleating site of the crystallization of the PBS/P3HB4HB (90/10) blend can be observed less than that of the neat PBS. ZnO nanoparticles was presented in the picture because ZnO was not molten at that temperature and ZnO nanoparticles acted as nucleating agents during PBS/P3HB4HB crystallization because ZnO had a hexagonal crystal structure with a closely packed lattice arrangement. This structure provides sites for the nucleation and growth of polymer. There were more and smaller spherulites comparing with those of PBS/P3HB4HB (90/10) blend .

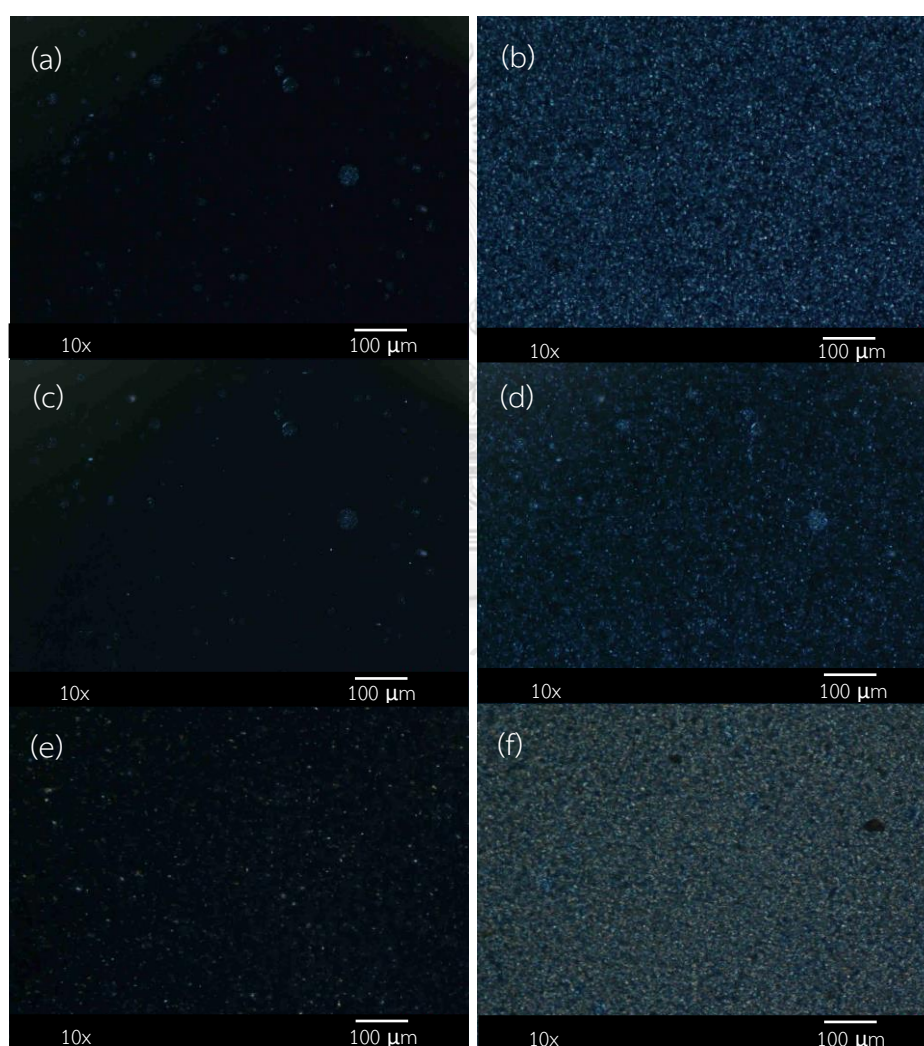


Figure 4.5 POM of the neat PBS at 95°C (a), neat PBS after 5 mins (b) PBS/P3HB4HB (90/10) blend, at 95 °C (c), PBS/P3HB4HB (90/10) blend after 5 mins (d) PBS/P3HB4HB/ZnO (90/10/2) blend, at 95 °C (e), and PBS/P3HB4HB/ZnO (90/10/2) blend after 5 mins (d)

4.3 Thermal properties of polymer films

The thermal properties of all polymer films were investigated by differential scanning calorimetry (DSC). As shown in Table 4.1, the glass transition temperature (T_g) of the neat PBS was not detected by DSC. The neat PBS showed double melting behavior. The first peak (T_{m1}) at 105.7 °C correspond to melting of the less ordered crystalline form. The second peak (T_{m2}) at 113.7 °C correspond to melting of ordered crystalline form. The neat P3HB4HB exhibited a T_g of -35.8 °C and a T_m of 142.4 °C. In the PBS/P3HB4HB (90/10) blend, the T_g and T_m did not show significant differences among the polymer blend. In Figure 4.6, two peaks were observed in the T_m of the polymer blend. Percentage of crystallinity (X_c) of the PBS/P3HB4HB (90/10) blend decreased from 48.30% to 30.06%, indicating increased molecular chain mobility in the polymer blend [2].

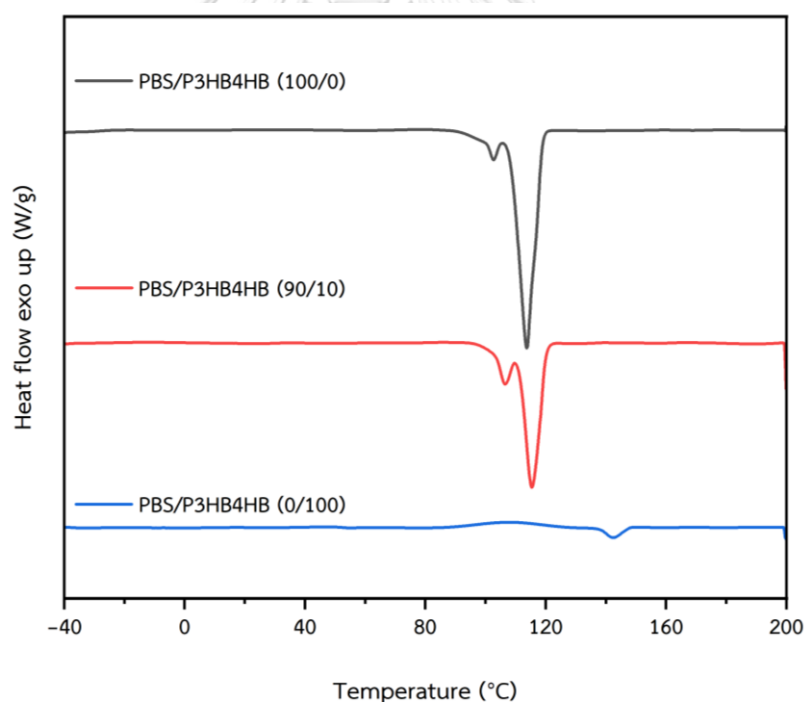


Figure 4.6 DSC Thermograms of the neat PBS, the neat P3HB4HB and PBS/P3HB4HB (90/10) blends.

Table 4.1 Thermal properties of all polymer films.

Polymer	T_g^a (°C)	T_g^b (°C)	T_m^{a1} (°C)	T_m^{a2} (°C)	T_m^b (°C)	X_c (%)
PBS/P3HB4HB (100/0)	N/A	-	105.7	113.7	-	48.30
PBS/P3HB4HB (90/10)	N/A	-34.4	106.3	113.0	143.2	30.06
PBS/P3HB4HB (0/100)	N/A	-35.8	-	-	142.4	1.75

^a PBS

^b P3HB4HB

The thermal properties of polymer films as shown in Figure 4.7, and Table 4.2, adding ZnO nanoparticles (0.5%, 1%, and 2%), the T_g and T_m did not show significant differences among the different ZnO nanoparticles content, but the significant effects on the X_c of polymer films. The X_c of polymer films when adding ZnO nanoparticles (0.5%, 1%, and 2%) increased from 30.06% to 49.79%, ZnO nanoparticles acted as nucleating agents indicating increased nucleating site in the polymer and correlated with the changes in POM [12].

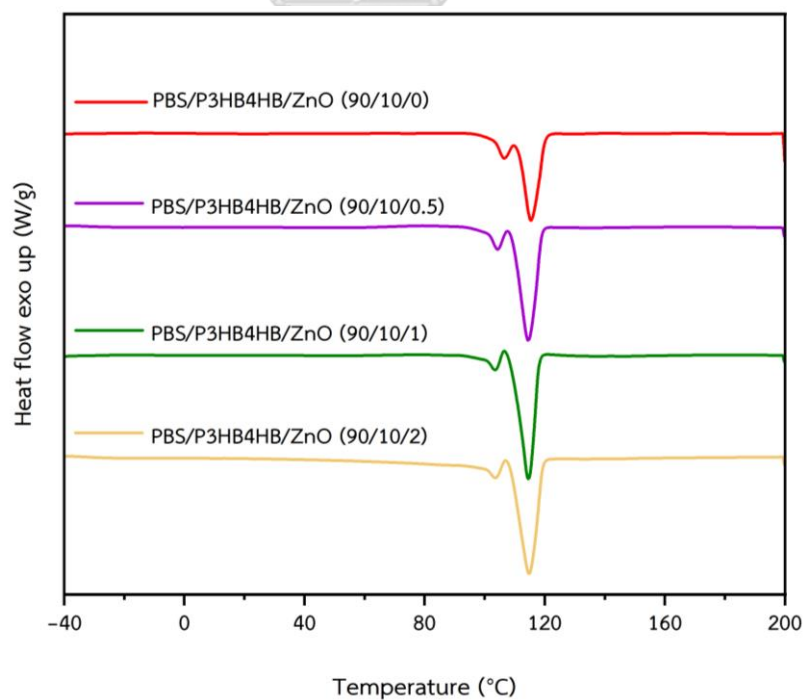


Figure 4.7 DSC Thermograms of the PBS/P3HB4HB (90/10) blend, PBS/P3HB4HB/ZnO (90/10/0.5), PBS/P3HB4HB/ZnO (90/10/1), and PBS/P3HB4HB/ZnO (90/10/2)

Table 4.2 Thermal properties of all polymer films.

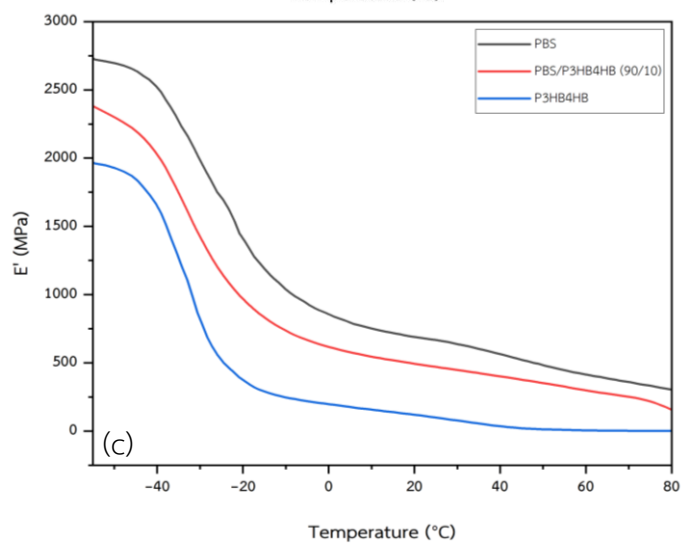
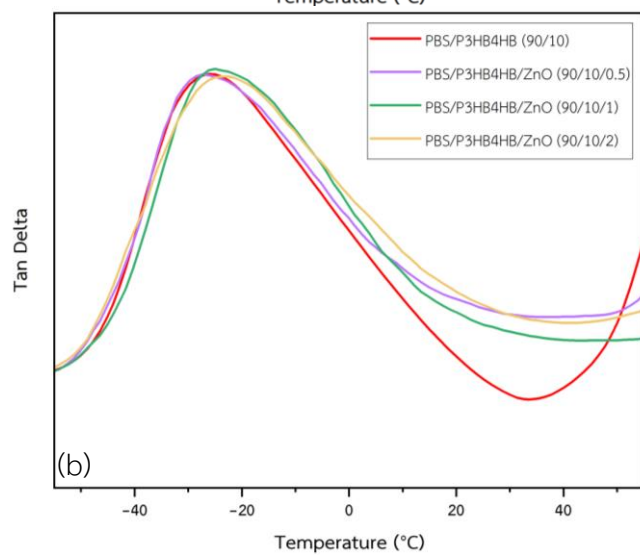
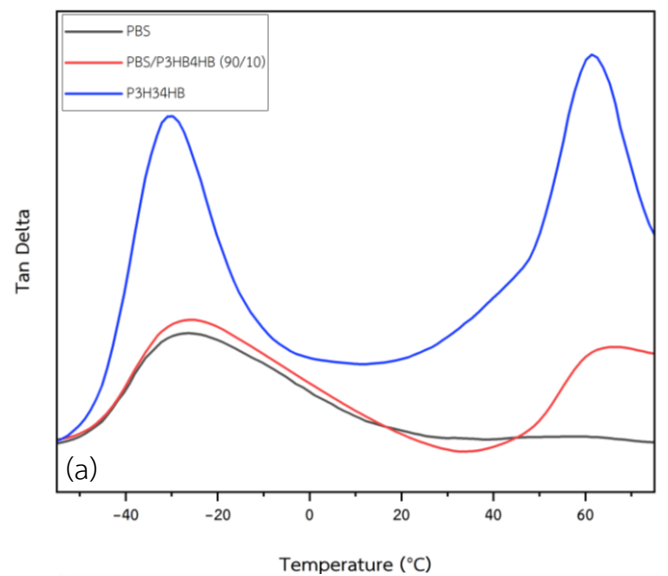
Polymer	T_g^a (°C)	T_g^b (°C)	T_m^{a1} (°C)	T_m^{a2} (°C)	T_m^b (°C)	X_c (%)
PBS/P3HB4HB (90/10)	N/A	-34.4	106.3	113.0	143.2	30.06
PBS/P3HB4HB/ZnO (90/10/0.5)	N/A	-33.2	105.3	114.1	142.2	45.17
PBS/P3HB4HB/ZnO (90/10/1)	N/A	-33.1	105.5	114.2	142.4	47.82
PBS/P3HB4HB/ZnO (90/10/2)	N/A	-33.2	106.7	114.4	142.4	49.79

^a PBS

^b P3HB4HB

4.4 Dynamic Mechanical properties

Dynamic mechanical analysis was performed by using a dynamic mechanical analyzer (DMA). As shown in Figure 4.8(a), $\tan\delta$ is the ratio between loss modulus (E'') and storage modulus (E'). The neat PBS showed only one glass transition peak (T_g) at -26.1 °C. The neat P3HB4HB had two glass transition peaks (T_g) at -34.3 °C and 60.1 °C, respectively. For PBS/P3HB4HB (90/10) blend showed two glass transition peaks at -26.6 °C and 60.3 °C, respectively. As a result, the T_g did not show significant differences among the polymer blend, which indicates PBS/P3HB4HB (90/10) blend is immiscible. As shown in Figure 4.8(b), for polymer blend with different ZnO nanoparticles contents, the addition of ZnO (1 and 2%) leads to a slight shift of glass transition temperature toward higher than PBS/P3HB4HB (90/10) blend due to the glass transition temperature is influenced by the mobility of chain segments within the amorphous regions, the addition of ZnO nanoparticles restricts chain mobility, consequently resulting in an elevation of the T_g [12]. When ZnO nanoparticles increase, the E' is increased. This improvement was related to the increase in the crystallinity and had strong interactions between ZnO and the C=O of the ester groups of the polymer blend [2, 6].



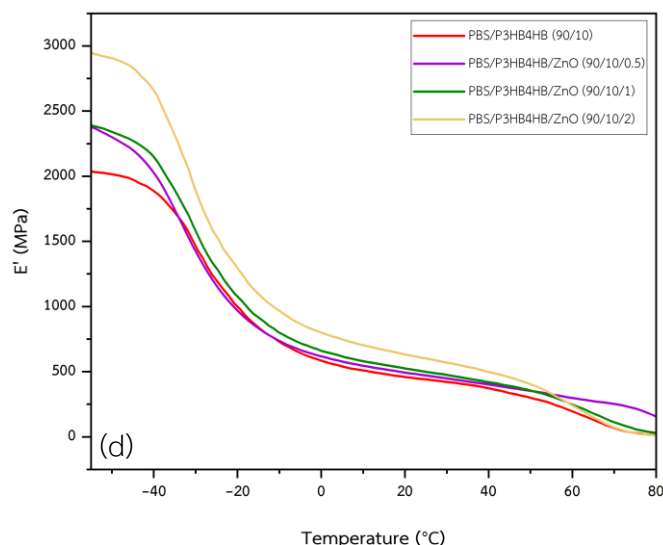


Figure 4.8 DMA measurements of the neat PBS, the neat P3HB4HB, PBS/P3HB4HB (90/10) blend (a and b) and PBS/P3HB4HB/ZnO; (a) $\tan\delta$ and (c and d) storage modulus (E') as a function of temperature

4.5 Mechanical properties of polymer films

The mechanical properties of all polymer films are shown by the stress-strain curves. The Figure 4.9, showed the behavior of the polymer blend when applying stress to the polymer, the initial point showed elastic deformation. In plastic deformation, stress was removed and strain wasn't returned to the initial point. After that, strain hardening occurred. As shown in Table 4.3, the tensile strength of the neat PBS and P3HB4HB were 30.88 and 6.82 MPa, respectively. The tensile strength of the PBS/P3HB4HB (90/10) blend was 26.65 MPa, that was lower than the neat PBS following by rule of mixing. The PBS/P3HB4HB (90/10) blend had higher elongation at break as compared to neat PBS. The reason for this is that the addition of P3HB4HB increased their flexibility [2].

Table 4.3 Mechanical properties of all polymer films.

Polymer	Young's modulus (MPa)	Tensile strength (MPa)	Elongation at break (%)	Toughness ($\text{J}\cdot\text{m}^{-3}$)
PBS/P3HB4HB (100/0)	475.76 ± 12	30.88 ± 2.7	10.48 ± 0.6	185.64 ± 2
PBS/P3HB4HB (90/10)	359.46 ± 14	26.65 ± 3.6	13.39 ± 1.3	225.18 ± 2
PBS/P3HB4HB (0/100)	216.82 ± 10	6.82 ± 0.4	17.71 ± 0.9	84.53 ± 2

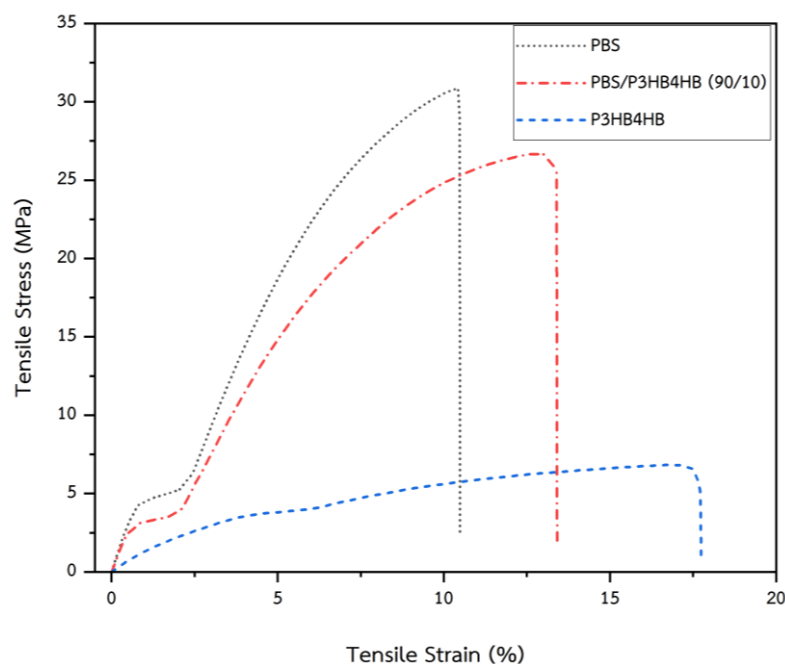


Figure 4.9 Stress-Strain curves of the neat PBS, the neat P3HB4HB and PBS/P3HB4HB (90/10) blends.

The mechanical properties of all polymer films are shown in Table 4.4, when ZnO nanoparticle increases, tensile strength is increased, the reason for this is ZnO nanoparticle obstructed chain mobility in the polymer films and had strong interactions between ZnO and the C=O of the ester groups of polymer blend [20, 7]. The Young's modulus was increased from 359.46 to 422.08 MPa, whose trends was similar to that of tensile strength. The elongation at break was slightly decreased when adding ZnO nanoparticles, the elongation at break was decreased from 13.39% to 13.01%. which could be due to the presence of ZnO could obstruct chain mobility and reduce their flexibility [20, 7]. The toughness of PBS/P3HB4HB/ZnO (90/10/0.5) was decreased due to the ZnO nanoparticle's heterogeneous phase dispersion and decreased interfacial adhesion [2]. The toughness of ZnO nanoparticles (1% and 2%) was agglomerated, which is attributed to adsorption energy [20].

Table 4.4 Mechanical properties of all polymer films.

Polymer	Young's modulus (MPa)	Tensile strength (MPa)	Elongation at break (%)	Toughness ($\text{J}\cdot\text{m}^{-3}$)
PBS/P3HB4HB (90/10)	359.46 ± 11	26.65 ± 1.1	13.39 ± 1.0	225.18 ± 8
PBS/P3HB4HB/ZnO (90/10/0.5)	396.96 ± 2	28.33 ± 2.5	10.85 ± 0.5	175.32 ± 8
PBS/P3HB4HB/ZnO (90/10/1)	408.77 ± 11	29.61 ± 1.0	12.66 ± 1.1	235.11 ± 10
PBS/P3HB4HB/ZnO (90/10/2)	422.08 ± 9	32.12 ± 1.6	13.01 ± 2.0	233.04 ± 10

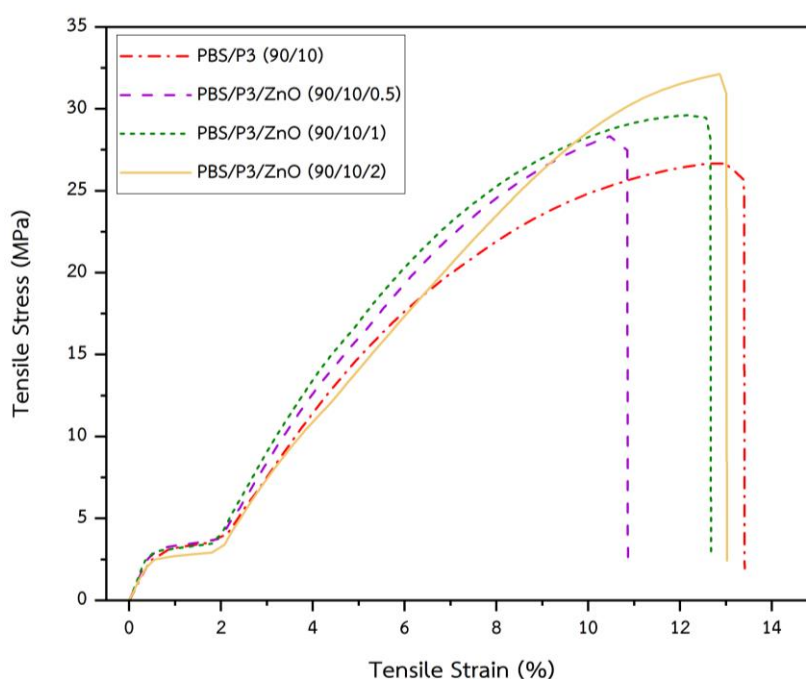


Figure 4.10 Stress-Strain curves of the PBS/P3HB4HB (90/10) blend, PBS/P3HB4HB/ZnO (90/10/0.5), PBS/P3HB4HB/ZnO (90/10/1), and PBS/P3HB4HB/ZnO (90/10/2)

4.6 Gas barrier properties of polymer films

Oxygen transmission rate (OTR) of all polymer films was measured by using an oxygen permeation analyzer. As can be seen in Figure 4.11(a), the OTR was decreased from 380.86 to 298.32 $\text{cc}/\text{m}^2\cdot\text{day}$. When the content of ZnO nanoparticles increased, the OTR was decreased because ZnO nanoparticles and crystallinity phase of polymer created a tortuous pathway for oxygen molecules to diffuse through films [6].

Water vapor transmission rate (WVTR) of all polymer films was measured by using a water vapor permeation analyzer. As can be seen in Figure 4.11(b), when adding ZnO nanoparticles, WVTR was decreased from 351.85 to 78.53 $\text{g}/\text{m}^2\text{-day}$, that showed ZnO improved barrier properties against water vapor. ZnO nanoparticles and crystal structure created a tortuous pathway for water vapor molecules, effectively reducing the WVTR. These improvements corresponded with the increased crystallinity with the ZnO loading, water vapor was unable to permeate the polymer crystallites [7].

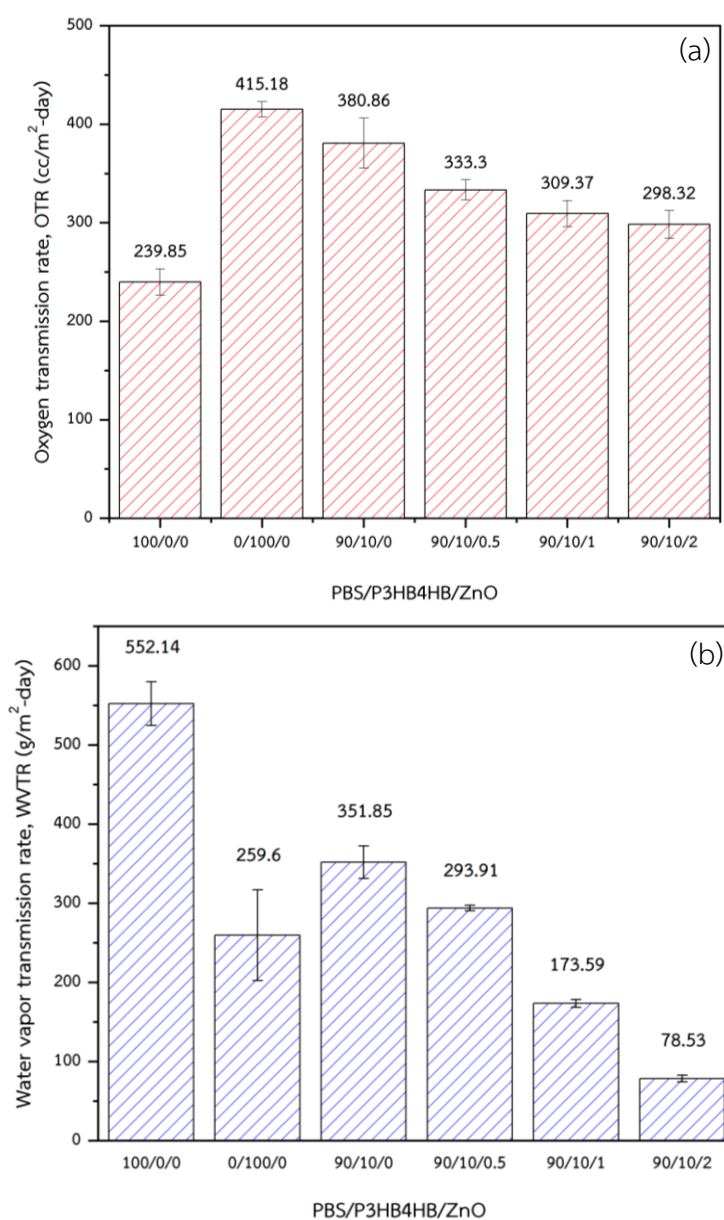


Figure 4.11 Oxygen and Water vapor transmission rate of all polymer s films.

CHAPTER 5

Conclusions

In this research, P3HB4HB was selected to blend with PBS with weight ratios of 90/10 and ZnO was selected as a nucleating agent to enhance the thermal, mechanical, morphological, and gas barrier properties of PBS/P3HB4HB blends. From the results, The FT-IR showed new absorption bands at 3140 cm^{-1} were attributed to hydrogen bonding between ZnO and polymer films. SEM showed ZnO particles which were dispersed in the polymer matrix. In the spherulite morphology, ZnO nanoparticles acted as nucleating agents, promoting the nucleation and growth of polymer crystallites. The percentage of crystallinity was increased, indicating increased nucleating site in the polymer s correlated to the spherulite morphology. When adding ZnO nanoparticles, it improved mechanical properties in terms of Young's modulus and tensile strength. In terms of barrier properties, ZnO nanoparticles decreased OTR and dramatically reduced WVTR. The results suggested that the presence of ZnO in PBS/P3HB4HB/ZnO films can improve the crystallinity, mechanical, and gas barrier properties of PBS.

Recommendation

1. To investigate the limitations of ZnO nanoparticles, suggested varying different amounts and particle sizes of ZnO nanoparticles.
2. In future work, the antimicrobial properties and UV-VIS characteristics of the films should be investigated to develop them for packaging applications.

REFERENCES

1. Bumbudsanpharoke N, Wongphan P, Promhuad K, Leelaphiwat P, Harnkarnsujarit N. Morphology and permeability of bio-based poly(butylene adipate-co-terephthalate) (PBAT), poly(butylene succinate) (PBS) and linear low-density polyethylene (LLDPE) blend films control shelf-life of packaged bread. *Food Control*. 2022;132.
2. Ayu RS, Khalina A, Harmaen AS, Zaman K, Isma T, Liu Q, et al. Characterization Study of Empty Fruit Bunch (EFB) Fibers Reinforcement in Poly(Butylene) Succinate (PBS)/Starch/Glycerol Composite Sheet. *Polymers (Basel)*. 2020;12(7).
3. Ahmad Thirmizir MZ, Mohd Ishak ZA, Mat Taib R, C. Kanapathi Pillai KSK, Salim MS, Hassan A, et al. The effects of melt grafted maleated polybutylene succinate on the properties of poly(hydroxybutyrate-co-hydroxyhexanoate)/polybutylene succinate blends. *Journal of Vinyl and Additive Technology*. 2021;27(3):567-88.
4. Rafiqah SA, Khalina A, Harmaen AS, Tawakkal IA, Zaman K, Asim M, et al. A Review on Properties and Application of Bio-Based Poly(Butylene Succinate). *Polymers (Basel)*. 2021;13(9).
5. Chen Z, Zhao Z, Hong J, Pan Z. Novel bioresource-based poly(3-Hydroxybutyrate-co-4-Hydroxybutyrate)/poly(LacticAcid) blend fibers with high strength and toughness via melt-spinning. *Journal of Applied Polymer Science*. 2020;137(32).
6. Luo R, Xu K, Chen G-Q. Study of miscibility, crystallization, mechanical properties, and thermal stability of blends of poly(3-hydroxybutyrate) and poly(3-hydroxybutyrate-co-4-hydroxybutyrate). *Journal of Applied Polymer Science*. 2007;105(6):3402-8.
7. Luo L, Wei X, Chen GQ. Physical properties and biocompatibility of poly(3-hydroxybutyrate-co-3-hydroxyhexanoate) blended with poly(3-hydroxybutyrate-co-4-hydroxybutyrate). *J Biomater Sci Polym Ed*. 2009;20(11):1537-53.
8. Diez-Pascual AM, Xu C, Luque R. Development and characterization of novel poly(ether ether ketone)/ZnO bionanocomposites. *J Mater Chem B*. 2014;2(20):3065-78.
9. Diez-Pascual AM, Diez-Vicente AL. ZnO-reinforced poly(3-hydroxybutyrate-co-3-

hydroxyvalerate) bionanocomposites with antimicrobial function for food packaging. *ACS Appl Mater Interfaces*. 2014;6(12):9822-34.

10. Chen H, Oveissi F, Daly S, Shahrabaki Z, Naficy S, Dehghani F. A green and biodegradable plasticizer from copolymers of poly (β -hydroxybutyrate-co- ϵ -caprolactone). *Journal of Applied Polymer Science*. 2022;139(22):52240.
11. de Beukelaer H, Hilhorst M, Workala Y, Maaskant E, Post W. Overview of the mechanical, thermal and barrier properties of biobased and/or biodegradable thermoplastic materials. *Polymer Testing*. 2022;116:107803.
12. Garcia-Garcia D, Quiles-Carrillo L, Balart R, Torres-Giner S, Arrieta PM. Innovative solutions and challenges to increase the use of Poly (3-hydroxybutyrate) in food packaging and disposables. *European Polymer Journal*. 2022:111505.
13. Kantor-Malujdy N, Skowron S, Michalkiewicz B, El Fray M. Poly (butylene-succinate)-based blends with enhanced oxygen permeability. *Materials Today Communications*. 2022;33:104306.
14. Na H, Huang J, Xu H, Liu F, Xie L, Zhu B, et al. Structure and Properties of PLA Composite Enhanced with Biomass Fillers from Herbaceous Plants. *Journal of Renewable Materials*. 2023;11(2):491-503.
15. Opálková Šišková A, Mosnáčková K, Musioł M, Opálek A, Bučková M, Rychter P, et al. Electrospun Nisin-Loaded Poly (ϵ -caprolactone)-Based Active Food Packaging. *Materials*. 2022;15(13):4540.
16. Pietrosanto A, Scarfato P, Di Maio L, Incarnato L. Development of PLA/PHB blown films with improved performance for food packaging applications. *Chemical Engineering Transactions*. 2021;87:91-6.
17. Lagarón JM, López-Rubio A, José Fabra M. Bio-based packaging. *Journal of Applied Polymer Science*. 2016;133(2):n/a-n/a.
18. Homklin R, Hongsriphan N. Mechanical and Thermal Properties of PLA/PBS Co-continuous Blends Adding Nucleating Agent. *Energy Procedia*. 2013;34:871-9.
19. Zhang X, Shi J, Zhou J, Nan J. Nucleation effect of cellulose nanocrystals/polybutylene succinate composite filler on polylactic acid/polybutylene succinate blends. *Polymer Bulletin*. 2021;79(7):5481-94.

20. Chuayjuljit S, Kongthan J, Chaiwutthinan P, Boonmahitthisud A. Poly(vinyl chloride)/Poly(butylene succinate)/wood flour composites: Physical properties and biodegradability. *Polymer Composites*. 2018;39(5):1543-52.
21. Threepopnatkul P, Wongnarat C, Intolo W, Suato S, Kulsetthanchalee C. Effect of TiO₂ and ZnO on Thin Film Properties of PET/PBS Blend for Food Packaging Applications. *Energy Procedia*. 2014;56:102-11.
22. Chaochanchaikul K, Sakulphaemaruehai C. Effect of nanoclay and nano-calcium carbonate content on the properties of polybutylene succinate/nanoparticle composites. *Journal of Plastic Film & Sheeting*. 2023;39(2):190-210.
23. Phothisarattana D, Wongphan P, Promhuad K, Promsorn J, Harnkarnsujarit N. Blown film extrusion of PBAT/TPS/ZnO nanocomposites for shelf-life extension of meat packaging. *Colloids Surf B Biointerfaces*. 2022;214:112472.
24. Qin YX, Wang C, Li KY, Jin BR, Chen YR, Ren L, et al. Fully biodegradable composites from poly (butylene succinate) modified with poly(3-hydroxybutyrate-co-4-hydroxybutyrate): fabrication and properties. *Journal of Polymer Research*. 2023;30(2).
25. <Thesis-2013-Duan.pdf>.
26. Tang Z, Fan F, Chu Z, Fan C, Qin Y. Barrier Properties and Characterizations of Poly(lactic Acid)/ZnO Nanocomposites. *Molecules*. 2020;25(6).
27. Channa IA, Ashfaq J, Gilani SJ, Shah AA, Chandio AD, Jumah MNb. UV Blocking and Oxygen Barrier Coatings Based on Polyvinyl Alcohol and Zinc Oxide Nanoparticles for Packaging Applications. *Coatings*. 2022;12(7).



จุฬาลงกรณ์มหาวิทยาลัย
CHULALONGKORN UNIVERSITY

VITA

NAME Sunisa Suwatthi

DATE OF BIRTH 6 March 1999

PLACE OF BIRTH Bangkok

INSTITUTIONS ATTENDED Science, Kasetsart University, Bangkok, Thailand

HOME ADDRESS 27/292 Moo.7 Khlong Hok, Khlong Luang, Pathum Thani
12120

